UNIVERSIDADE DA BEIRA INTERIOR
Ciências da Saúde

Modelos de cultura celular para rastreio de fármacos

Marco António Paulo de Carvalho

Dissertação para obtenção do Grau de Mestre em
Ciências Biomédicas
(2º ciclo de estudos)

Orientador: Professor Doutor Ilídio Joaquim Sobreira Correia
Co-orientador: Mestre Elisabete Cristina da Rocha Costa

Covilhã, outubro de 2016

List of Publications

Articles in peer reviewed international journals:

Carvalho, M. P., Costa, E. C., Miguel, S. P., Correia, I. J., *Tumor spheroid assembly on hyaluronic acid-based structures: A review*. Carbohydrate Polymers, 2016. 150: 139-148.

Carvalho, M. P., Costa, E. C., Correia, I. J., *Assembly of breast cancer heterotypic spheroids on Hyaluronic Acid coated surfaces.* Journal of Biomolecular Screening, submitted.

Costa, E. C., Moreira, A. F., de-Melo, D., Gaspar, V. M., Carvalho, M. P., Correia, I. J., *3D Tumor Spheroids: An overview on tools and techniques used for their analysis*. Biotechnology Advances, submitted.

Poster communications:

Carvalho, M. P., Costa, E. C., Correia, I. J., *Assembly of breast cancer spheroids*, XI Annual CICS Symposium, July 1st 2016, Faculty of Health Sciences, Universidade da Beira Interior, Covilhã, Portugal. **Best poster award.**

Carvalho, M. P., Costa, E. C., Correia, I. J., *Hyaluronic acid biomaterial application in breast cancer spheroids assembly,* V Encontro Nacional de Estudantes de Materiais (ENEM), September 29 th, Universidade da Beira Interior, Covilhã, Portugal.

“Por vezes sentimos que aquilo que fazemos não é senão uma gota de água no mar. Mas o mar seria menor se lhe faltasse uma gota.”

Madre Teresa de Calcutá

Dedication

To my parents, sister and girlfriend…

Acknowledgments

Firstly, I would like to thank to my supervisor Professor Ilídio Correia for the opportunity to develop this project with him and his group. I am also grateful for his support, criticism and guidance that made me grow up as a professional and as a person. Furthermore, I would like to thank him for providing all necessary conditions for the development of this project. It was a privilege to work with him.

I also would like to express my gratitude to my co-supervisor and friend Elisabete Costa for all the knowledge that she shared with me and for all the support in the hard moments. I thank to her for believing in me and for helping me to be the professional and the person that I am today. There are no words to express my gratitude but I just want to thank her for be the person that "was always there".

I have to thank to my group colleagues for being always ready to help and for the good moments that they have promoted. In special, I would like to thank to Sónia Miguel for the help in the acquisition of scanning electron microscopy images. I thank her for the friendship and for all the support and help that she gave to me.

I would like to thank to my friends Daniela Figueira, Kevin de Sá and Luís Xavier for having appeared in my life and accompanying me during my academic life. They gave me the strength to get here.

Finally, I have to thank to my family members and to my girlfriend Céline da Silva for all the patience, support and encouragement. I thank them for helping me to surpass every challenge and for making my life so special.

Resumo

A cultura de células em duas dimensões (2D) é a principal metodologia utilizada para o rastreio de agentes terapêuticos anticancerígenos. No entanto, quando os modelos celulares em 2D são utilizados, a arquitetura dos tumores nativos não é reproduzida na sua plenitude, levando, em alguns casos, a uma previsão pouco precisa da resposta das células aos fármacos. Por outro lado, existe a necessidade de reduzir a utilização de modelos animais em laboratório, uma vez que estes têm associados problemas económicos e éticos. Para superar as limitações associadas aos modelos celulares produzidos em 2D e aos ensaios *in vivo*, os investigadores começaram a efetuar o crescimento de células em três dimensões (3D) com o objetivo de reproduzir *in vitro* a estrutura 3D dos tumores sólidos. Uma das técnicas mais utilizadas para a produção destes agregados celulares 3D, também conhecidos como esferoides, é a técnica de sobreposição líquida (*Liquid Overlay Technique – LOT*), na qual as células são forçadas a agregar devido à sua limitada adesão a certos biomateriais, geralmente agarose ou agar. No entanto, estes biopolímeros não têm a capacidade de interagir com as células cancerígenas nem de estabelecer interações semelhantes às que ocorrem entre as células e a matriz extracelular (MEC) nos tumores sólidos, que ativam as vias de sinalização celular reguladoras do comportamento das células tumorais. Com o intuito de mimetizar não só a estrutura 3D mas também as interações MEC que ocorrem nos tumores, têm sido produzidos modelos 3D nos quais as células interagem com componentes da MEC. Um dos biomateriais que tem sido usado com este objetivo é o ácido hialurónico (AH). Este composto é um dos principais componentes da MEC dos tumores, evita a adesão celular e tem um papel essencial na progressão do cancro. No presente estudo foi pela primeira vez otimizado o revestimento de superfícies com AH para a produção de forma reprodutível de esferóides heterotípicos do cancro da mama. Os resultados obtidos revelaram que as superfícies revestidas com AH permitem a produção de esferóides que reproduzem a estrutura 3D e a heterogeneidade celular encontrada nos tumores sólidos. Por outro lado, é possível controlar o tamanho, forma e número de esferóides produzidos alterando a concentração de AH e o número inicial de células semeadas. Em suma, os esferóides aqui produzidos em superfícies revestidas com AH representam uma grande melhoria para o futuro desenvolvimento de terapias anticancerígenas.

Palavras-chave

Ácido hialurónico; Cancro da mama; Esferóides tumorais; Matriz extracelular tumoral; Técnica de sobreposição líquida.

Resumo Alargado

As terapias anticancerígenas atuais, tais como a quimioterapia, radioterapia e cirurgia são conhecidas por terem uma eficácia terapêutica limitada e desencadearem efeitos secundários nos pacientes. Estas limitações exigem o desenvolvimento e otimização de novas abordagens terapêuticas. No entanto, para a sua validação e aplicação em contexto clínico, estas necessitam de ser previamente testadas em modelos capazes de representar o mais fielmente possível a complexidade dos tumores sólidos que afetam o ser humano. Por norma, os modelos animais (ex. ratos, porcos e macacos) são aqueles que podem reproduzir de forma mais fiel os tumores sólidos humanos. No entanto, a utilização de animais de laboratório está associado a problemas éticos, legais e económicos. De forma a contornar estes problemas, têm sido usados modelos de culturas celulares produzidos *in vitro*.

Até aos dias de hoje a cultura de células em 2D, ou seja, o crescimento de células em monocamada, é a principal plataforma usada para a avaliação de agentes anticancerígenos. Esta prática permite a avaliação de diferentes formulações terapêuticas de forma controlada, reprodutível e com baixos custos associados. No entanto, tem sido constatado que os modelos 2D não permitem prever com exatidão o efeito terapêutico de fármacos em humanos. Tal deve-se ao facto destes modelos serem incapazes de mimetizar a estrutura 3D dos tumores e a sua organização celular. Desta forma, os investigadores têm procurado desenvolver modelos 3D de culturas celulares, tal como os esferóides, que conseguem mimetizar as propriedades dos tumores.

Os esferóides são agregados celulares 3D que mimetizam várias propriedades dos tumores sólidos, tais como as interações célula-célula, organização celular, expressão de genes e resistência a fármacos. Por outro lado, os esferóides podem ser constituídos por diferentes tipos de células, como as células cancerígenas e células do estroma, que permitem reproduzir a heterogeneidade celular encontrada nos tumores.

Na atualidade, estão a ser desenvolvidas várias técnicas para a produção de esferóides, tais como *Hanging Drop* e *LOT*. Esta última, já foi anteriormente otimizada pelo nosso grupo para a produção de esferóides tumorais da mama. O seu processo de produção envolve a cultura de células sobre biomateriais não adesivos, tais como a agarose. Nestas condições as interações entre as células são privilegiadas, uma vez que as células não conseguem aderir ao biomaterial. Desta forma, as células formam agregados (esferóides). Contudo, a agarose não tem a capacidade de interagir com as células, nem tão pouco de ativar vias de sinalização celulares que são características dos tumores. Devido a este facto, tem-se procurado utilizar novos biomateriais não adesivos para a produção de esferóides pela técnica de *LOT*.

O AH é um dos materiais não adesivos e um dos principais constituintes da MEC dos tumores sólidos. No microambiente tumoral o AH interage com os recetores existentes nas membrana citoplasmática das células, tais como o CD44, promovendo desta forma a transdução de sinais intracelulares. Este biomaterial contribui não só para a progressão do tumor, mas também para os mecanismos de resistência a fármacos que as células cancerígenas apresentam.

No trabalho de investigação apresentado nesta tese foi desenvolvido e otimizado, pela primeira vez, a produção de esferóides heterotípicos do cancro da mama em superfícies revestidas com AH. Para além disso, foi também estudado o efeito da concentração do revestimento e do número inicial de células semeadas na produção de esferóides. A heterogeneidade celular do tumor foi também replicada através da utilização de diferentes rácios de células cancerígenas/células normais.

Os esferóides produzidos foram analisados através de microscopia ótica, microscopia eletrónica de varrimento e microscopia confocal. Os resultados obtidos demonstraram que as células presentes nos esferóides apresentavam uma organização 3D e que estas estabeleceram interações físicas entre si. Por outro lado, foi também foi possível observar que os esferóides possuíam um núcleo denso e necrótico rodeado de células em proliferação, tal como é observado nos tumores sólidos do cancro da mama. Por último, constatou-se que o tamanho e esfericidade dos agregados celulares são influenciados pela concentração de AH usado no revestimento e pelo número inicial de células semeadas em cada poço. Os esferóides com maior tamanho e esfericidade foram produzidos nas superfícies com a maior concentração de AH e com o maior número de células.

Com base nos resultados obtidos, espera-se que os esferóides produzidos em superfícies revestidas com AH possam ser uma grande mais valia para o desenvolvimento e otimização de terapias antitumorais devido ao seu baixo custo, facilidade de produção e capacidade para mimetizar várias características que os dos tumores sólidos da mama apresentam.

Abstract

Two-dimensional (2D) cell culture is the prime methodology used, for screening anticancer therapeutics. However, when 2D cellular models are used, the architecture of native tumors is not fully represented, leading in some cases to an unsuccessful prediction of cancer cells response to drugs. On the other hand, there is a need to reduce the use of animal research models once they have economical and ethical problems associated. To overcome the limitations associated to 2D cell culture models and *in vivo* assays, the researchers started to perform cell growth in three-dimensions (3D), for reproducing *in vitro* the 3D structure of solid tumors. One of the most applied techniques to produce these 3D cellular aggregates, also known as spheroids, is Liquid Overlay Technique (LOT), in which cells are forced to aggregate due to their limited adhesion to certain biomaterials, usually agarose or agar. However, these biopolymers cannot interact with cancer cells, neither establish interactions that are similar to those occurring between cells and extracellular matrix (ECM) in solid tumors, which are responsible for the activation of cellular signaling pathways that regulate cancer cells behavior. In order to mimic not only the 3D structure but also the cell-ECM interactions that occur in tumors, it has been proposed the production of 3D models in which cells can interact with tumor ECM components. One of the biomaterial that has been used with this objective is the hyaluronic acid (HA). This compound is one of the main constituents of tumor ECM, it avoids cell adhesion and it has an essential role in cancer progression. In this work it was optimized, for the first time, the coating of surfaces with HA that were used for the production of reproducible heterotypic breast cancer spheroids. The obtained results revealed that the HA coated surfaces allow the production of spheroids that reproduce the 3D structure and the cellular heterogeneity presented by breast solid tumors. Furthermore, it was possible to control the size, shape and number of spheroids produced by changing the HA concentration and the number of cells initially seeded. Overall, these breast cancer spheroids assembled on HA-coated surfaces represent a huge improvement for the future development of anticancer therapies.

Keywords

Breast cancer; Hyaluronic acid; Liquid Overlay Technique; Tumor extracellular matrix; Tumor spheroids.

Table of Contents

List of Figures

List of Tables

Chapter I

List of Acronyms

ABC transporter	Adenosine triphosphate-binding cassette transporter
ABCG2	Adenosine triphosphate-binding cassette sub-family G member 2
AC	Acrylate groups
AKT	Protein kinase B
AO	Acridine orange base
ATP	Adenosine triphosphate
BAD	B-cell lymphoma 2-associated death protein
Bcl-2	B-cell lymphoma 2
BCRC5	Baculoviral inhibitor of apoptosis repeat-containing 5
bFGF	Basic fibroblast growth factor
Cad11	Cadherin 11
CD133	Cluster of differentiation 133
CD44	Cluster of differentiation 44
CLSM	Confocal laser scanning microscopy
CSC	Cancer stem cell
c-Src	Proto-oncogene tyrosine-protein kinase
CXCR4	C-X-C chemokine receptor type 4
DMEM-F12	Dulbecco's Modified Eagles's Medium F-12
ECM	Extracellular matrix
EDC	Ethyl (dimethylaminopropyl) carbodiimide
EDTA	Ethylenediaminetetraacetate
EMT	Epithelial-mesenchymal transition
ERK1	Extracellular signal-regulated kinase 1
ERK2	Extracellular signal-regulated kinase 2
FAK	Focal adhesion kinase
FBS	Fetal bovine serum
FKHR	Forkhead homolog in rhabdomyosarcoma

GBM	Human glioblastoma multiforme
GFAP	Glial fibrillary acidic protein
HA	Hyaluronic acid
HIF-1α	Hypoxia-inducible factor 1-α
HMW	High molecular weight
IC50	Half maximal inhibitory concentration
IL-6	Interleukine 6
LMW	Low molecular weight
LOT	Liquid Overlay Technique
MAPK	Mitogen-activated protein kinase
MDR1	Multi-drug resistance gene 1
MDR2	Multi-drug resistance gene 2
MeHA	Methacrylated hyaluronic acid
MMP2	Matrix metalloproteinase 2
MMP9	Matrix metalloproteinase 9
MSC	Mesenchymal stem cell
NCI	National Cancer Institute
NHDF	Normal human dermal fibroblast
NHS	N-hydroxysuccinimide
Oct4	Octamer-binding transcription factor 4
o-HA	Hyaluronic acid oligosaccharide
p53	Tumor supressor p53
PBS	Phosphate-buffered saline solution
PCL	Polycaprolactone
PCR	Polymerase chain reaction
PDX	Patient-derived xenografts
PEC	Polyelectrolyte complexes
PFA	Paraformaldehyde
PI	Propidium iodide

PI3K	Phosphatidylinositol 3 kinase
Rac1	Ras-related C3 botulinum toxin substrate 1
RCC	Renal clear cell carcinoma
RGD	Arginine-glycine-aspartic acid
RHAMM	Receptor for hyaluronan-mediated motility
RhoGTPase	Rho family small GTPases
RT	Room temperature
SEM	Scanning electron microscopy
SF	Silk fibroin
SH	Reactive thiols
Sox2	Sex determining region Y-box 2
Sox9	Sex determining region Y-box 9
TGF-ß1	Transforming growth factor ß1

Chapter I

Introduction

1. Introduction

Conventional cancer treatments (*e.g.*, chemotherapy, radiotherapy and surgery) are known for triggering side effects and, in some types of cancer, for displaying a limited therapeutic outcome [1]. Such limitations demand the development of new therapeutic approaches. To accomplish such objective, it is pivotal to develop new accurate *in vitro* tumor models that can provide reliable experimental evidences on drug screening in a short period of time and with reduced costs. Nowadays, 2D cell culture is still the standard procedure used to evaluate the effectiveness and safety of new pharmaceutical compounds during the pre-clinical assays, since this type of cell culture is easy to handle, fast to grow and cost-effective. Nevertheless, cell growth on flat surfaces does not completely represent the cell-cell and cell-extracellular matrix (ECM) interactions that occur in real tumors, neither the proliferation, survival, migration or invasion capacity exhibited by cancer cells [2]. Furthermore, the United States National Cancer Institute (NCI) considered that various cells of NCI-60 (group of various cell lines recurrently used by researchers around the world for drug-screening purposes) are adapted to grow on plastic cell culture materials in conditions that differs from their native origin leading to an altered cellular behavior and gene expression [3]. As a consequence, some 2D cell culture assays provide inaccurate and wrong predictive data about the activity of bioactive molecules when compared to the *in vivo* counterpart [4].

Due to that, NCI is developing newer tumor models, such as patient-derived xenografts (PDX) that are obtained by implanting pieces of human tumors into mice [3]. Notwithstanding, is still necessary to develop optional platforms for the evaluation of therapeutics that avoid the ethical and legal issues related with the use of animals in laboratory. Accordingly, researchers are currently developing 3D cell culture models, like spheroids, that are able to better reproduce the structural organization presented by solid tumors. The similarities found between spheroids and solid tumors include growth kinetic rates, gene expression levels, and cell layers arrangement (including proliferative, quiescence and necrotic strata) (Figure 1) (reviewed in [5, 6]). These 3D cellular aggregates also display nutrients, gases (O_2 and CO_2) and pH gradients as well as resistance to therapeutics, likewise solid tumors. Furthermore, a limited penetration of therapeutic molecules (Figure 1) and an up-regulated survival and anti-apoptotic proteins expression (*e.g.*, B-cell lymphoma 2 (Bcl-2) and survivin) are additional features of spheroids [7].

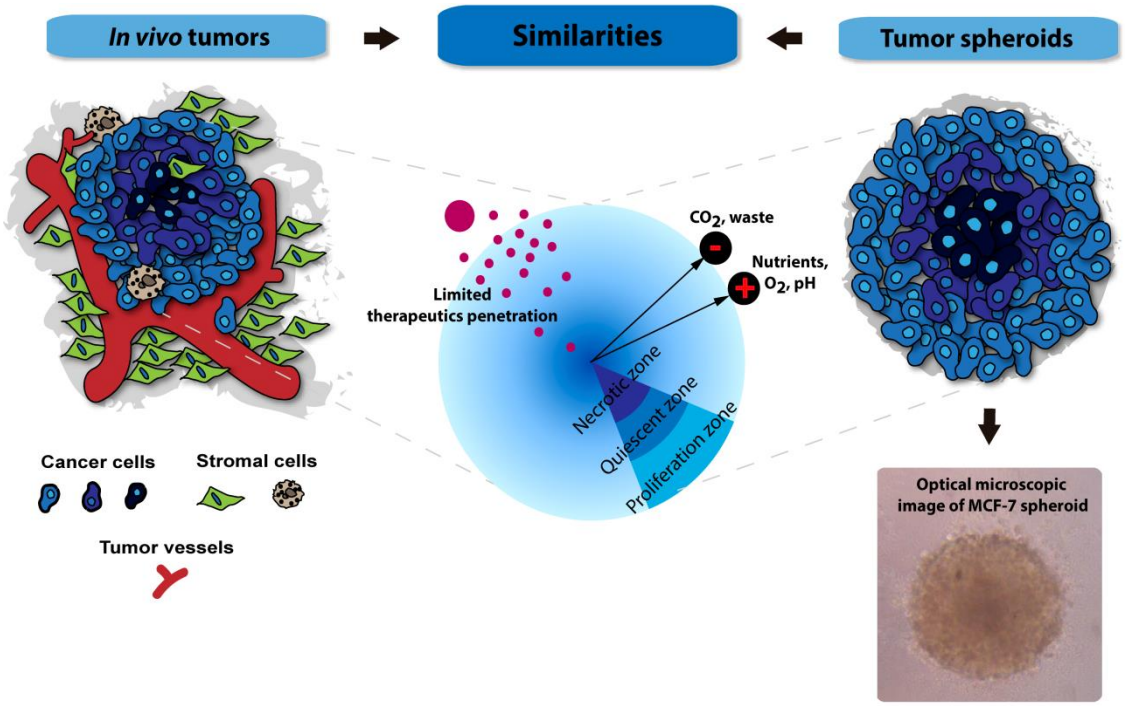

Figure 1. Representation of structural features that are common to tumor spheroids and solid tumors. Tumor spheroids are organized in three distinct layers of cells (necrotic, quiescent and proliferative) as in real tumors. Such structural arrangement is a consequence of nutrients, gases, pH and waste gradients. Additionally, spheroids also display a limited penetration for therapeutic molecules.

Up to now, Gyratory Rotation [8], Hanging Drop [9], Liquid Overlay Technique (LOT) [10] and Microfluidics [11] have been used to produce spheroids in a quickly and reproducible way. All these techniques allow the production of 3D cellular aggregates constituted by cancer cells or other type of cells (*e.g.*, fibroblast, hepatocytes, stem cells). However, spheroids produced by these techniques display a low presence of some ECM components, as well as cell-ECM interactions. Therefore, a huge effort is currently being done for these 3D models reproduce the complex tumor ECM, since the mechanisms that regulate the cancer cells metabolism and also their response to therapeutic molecules can be modulated by the ECM and cells-ECM cross talk.

In previous studies, it has been reported that some ECM components are able to modulate cancer cells activity [12-21]. HA, also known as hyaluronan or hyaluronate, is a non-sulfated glycosaminoglycan of the proteoglycan complex found in the ECM (Figure 2) [12]. The higher content of HA present in cancer microenvironment favors tumor progression, leading to a reduced patient life expectancy [13]. The role of HA in cancer progression results from the interaction of this molecule with cell surface receptors that will promote the transducing of intracellular signals involved in cells differentiation, survival, proliferation, migration, angiogenesis and resistance to therapeutic molecules (as it will be discussed hereafter) [15, 17, 22, 23].

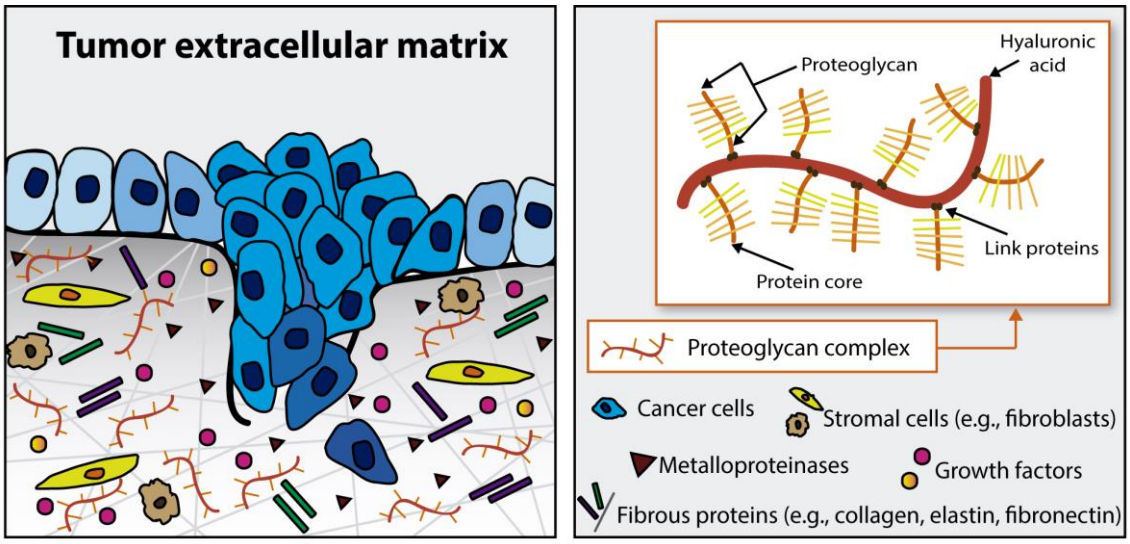

Figure 2. Schematic representation of the tumor ECM organization and composition. This ECM is mainly composed by a complex mixture of macromolecules, such as fibrous proteins (collagens, elastins, fibronectins and laminins) and proteoglycans. HA, which is a main constituent of proteoglycans, is widely present in the ECM of different tumors.

In addition, cells display a reduced adhesion to HA [24-26]. This property favors tumor spheroids assembly, considering that when cells are seeded on poor adhesive biomaterials the establishment of few cell-biomaterial physical interactions results in cellular aggregates [6].

Therefore, HA-based structures, such as solid scaffolds, fibers, hydrogels, microbeads and HA coated surfaces have been produced for optimizing spheroids production. Tumor spheroids produced in HA-based structures are able to reproduce the 3D architecture of tumors and also mimic the cell-HA signaling existent in the tumor microenvironment. Such features are crucial when these models are aimed for cancer therapeutic screening purposes.

1.1. HA role in tumor microenvironment

In the literature, there are several studies highlighting the HA effects on cancer cells behavior, which are prompted by HA binding to cancer cell surface receptors, like glycoprotein CD44 and hyaluronan-mediated motility (RHAMM), as demonstrated in Figure 3.

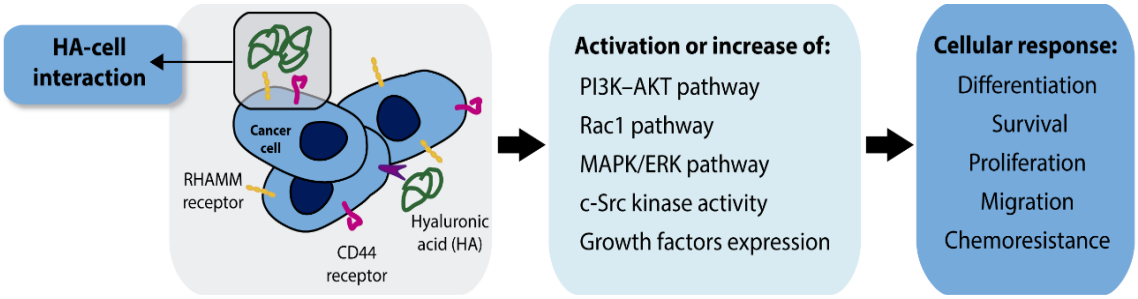

Figure 3. HA interaction with cell surface receptors (CD44 and RHAMM) influences cellular differentiation, survival, proliferation, migration and its chemoresistance by activating intracellular signaling pathways.

Ahrens *et al*. evidenced that melanoma cells cultured with HA have higher growth rate. Such result was explained by the establishment of HA-CD44 interactions, which enhanced the release of autocrine growth factors, such as basic fibroblast growth factor (bFGF), that are involved in tumor proliferation and angiogenesis [14]. In another study performed by Ghatak and co-workers, it was proposed that HA may be involved in the activation of phosphatidylinositol 3 kinase - protein kinase B (PI3K–AKT) pathway in lung carcinoma cells [27]. PI3K–AKT is a via well known by playing a primary role in cancer cells survival, growth and proliferation, by suppressing pro-apoptotic factors (*e.g.*, BAD and procaspase -9 and -3), inhibiting p53 regulated processes, activating the expression of proliferative and anti-apoptotic genes (*e.g.*, Bcl-2 and surviving), stimulating cell cycle progression (reviewed in [28, 29]).

Additionally, HA is involved in tumor angiogenesis, migration and invasion. Bourguignon *et al*. showed that HA-CD44 cross-talk leads to the phosphorylation and activation of proto-oncogene tyrosine-protein kinase Src (c-Src) [30]. Once activated, c-Src phosphorylates transcription factor - twist, promoting cell survival, angiogenesis, migration, metastasis and chemoresistance [30, 31]. Other studies demonstrated that HA interaction with CD44 and RHAMM may increase cancer cell motility and invasion potential, through the activation of extracellular signal-regulated kinases (ERK1 and ERK2) and Rac1 pathways [16, 21, 32-34]. In addition, the overexpression of enzymes involved in ECM degradation, like matrix metalloproteinases (*e.g.*, MMP9 and MMP2) may also occur [21, 34].

In other studies, it was also described that the inhibition of HA synthesis or HA receptors expression leads to a lower resistance of cancer cells to a particular therapy (reviewed by Lokeshwar *et al*. [35]). In fact, Misra *et al*. stated that HA-CD44 binding may adjust the activity of multidrug resistance proteins (P-glycoprotein and multidrug resistance-associated protein 2), which are involved in drug efflux from cells, resulting in a reduced therapeutic effectiveness [36].

Others researchers have demonstrated that when cells are cultured in the presence of HA they express stem-like markers (*e.g.*, octamer-binding transcription factor 4 (Oct4), sex determining region Y-box 2 (Sox2), Nanog, ATP-binding cassette transporters (ABC transporters)) [37-39]. Such data, supports the involvement of HA in the maintenance of cells stem cell-like phenotype, when cultured *in vitro*, which can contribute to tumor multidrug resistance [40].

Table 1 summarizes different studies published in the literature, where the HA influence on cancer cells proliferation, survival, invasiveness, migration, metastasis, chemoresistance and stem-like profile was described.

Table 1. Summary of the different studies where the influence of HA on cancer cells behavior was evaluated.

Cancer cell behavior	Cancer type	*In vitro* model	Observations	Ref.
Adhesion	Fibrosarcoma	2D HT-1080 cell culture	• HA interaction with RHAMM receptor and subsequent activation of FAK and ERK 1/2 signaling pathways affects cell adhesion.	[16]
Invasion	Glioblastoma	U87MG, U251MG and U373MG cells culture in 2D and in Boyden chambers	• HA induced the invasion capacity of glioma cells by the induction of MMP9 through the FAK-ERK 1/2 signaling pathway.	[34]
	Lung cancer	QG90 cell culture in 2D and in Boyden chambers	• HA-CD44 interaction controls the secretion of MMP2 in the cell culture medium; • Treatment of cells with anti-CD44 blocks the HA-dependent activation of cells invasiveness.	[21]
	Breast cancer	2D MDA-MB-231 and MCF-7 cell culture	• RHAMM and CD44 promote sustained ERK1,2 activities in the cytoplasm, leading to high basal motility of invasive breast cancer cells.	[32]
Metastasis	Melanoma	2D B16-F1 cell culture	• Cells with higher pericellular HA have a higher potential to form metastases than cells with low content of HA at their surface.	[20]
	Bone metastases from renal cell carcinoma	2D and 3D cells culture of 786-O RCC in a HA hydrogel-based culture system	• Cells cultured in 3D (using an HA-based hydrogel) present a higher expression of cell-cell adhesion molecules (*e.g.*, cadherin 11), angiogenesis (*e.g.*, HIF-1α) and osteolytic (*e.g.*, interleukin 6) factors than those cultured in 2D.	[41]
Migration	Breast cancer	2D SP1 cell culture	• HA binding to CD44 regulates oncogenic signaling required for RhoGTPase activation and cytoskeleton-mediated tumor cell migration.	[33]
	Ovarian cancer	2D SK-OV-3.ipl cell culture	• HA binding to CD44 activates c-Src kinase that phosphorylates cytoskeleton proteins, like cortactin, that are involved in cancer cells migration.	[42]
	Breast cancer	2D MDA-MB-231 cell culture	• HA/CD44-mediated tumor invasion and also the formation of metastasis through c-Src phosphorylation.	[30]
Proliferation	Melanoma	2D HT144 cell culture	• HA interaction with CD44 receptor stimulates the expression of autocrine growth factors (TGF-β1 and bFGF) that induce cells proliferation.	[14]
	Pleural mesothelioma	2D ACC-MESO-1 and 921MSO cells culture	• Cells treated with HA displayed an enhanced proliferation and invasion potential in relation to non-treated cells; • CD44 silencing reduced the effect of HA treatment on cells proliferation.	[43]

Stem-like	Glioblastoma	3D U-118 MG cell culture in HA-chitosan scaffold	• Cells cultured on HA-chitosan scaffold show higher expression of stem-like markers, such as CD44, nestin, musashi-1, GFAP, ABCG2 and HIF-1α in comparison with those cultured in 2D; • Cells demonstrate a higher invasive potential and a higher resistance to Doxorubicin and Temozolomide due to their increased expression of ABCG2 drug efflux transporter.	[38]
	Lung cancer	3D aggregates of A549 and H1299 cells cultured in surfaces coated with chitosan and HA	• Cells cultured with HA have a higher expression of stem-like and epithelial-mesenchymal transition (EMT) markers (Nanog, Sox2, CD44, CD133, N-cadherin and Vimentin); • Cells also displayed a higher invasive activity and a multidrug resistance by the upregulation of MMP2, MMP9, BCRC5, Bcl2, multi-drug resistance gene (MDR1) and ABCG2.	[39]
Survival	Myeloma	2D myeloma cell culture isolated from patients	• HA acts as a survival and proliferative factor through an IL-6 autocrine pathway.	[19]
	Lung carcinoma	2D LX 1 cell culture	• HA oligomers suppressed the PI3K-AKT pathway in cells, leading to the activation of pro-apoptotic mediators (BAD and FKHR) and increased activity of the apoptotic effector (caspase-3).	[27]
Therapeutics resistance	Breast cancer	2D MCF-7/Adr cell culture	• Cells treated with o-HA demonstrate a suppression of both PI3K and mitogen-activated protein kinases (MAPKs) pathways. This results in an increase of cancer cells sensitivity to Doxorubicin.	[18]
	Breast cancer	2D MCF-7/Adr cell culture	• HA interferes with PI3K pathway and promotes the expression of MDR1.	[44]
	Head and neck squamous cell carcinoma	2D SCC-4 cell culture	• In the absence of HA, Cisplatin is able to inhibit tumor cell growth; • The addition of HA to the cell culture resulted in a 5-fold reduction of the ability of Cisplatin to cause cell death, suggesting that HA is involved in the mechanism that confers to cells resistance to this drug.	[45]
	Lung cancer	2D NCI-H322 cell culture	• MDR2 expression was induced in cells cultured with HA.	[46]
	Lung cancer and brain metastasis	2D and 3D H460M, NCI-H460 and SA87 cells culture	• The 5-fluorouracil and Doxorubicin IC_{50} were higher for all cells when they were cultured in HA-hydrogel; • HA is able to increase the cancer cell survival through PI3K- and MAPK-dependent stimulation of MDR.	[47]

1.1.1. HA molecular weight influence on cell signaling and tumorigenesis

HA size range may vary from few disaccharide repeats in length to million Da. HA over 1 million of Da is considered high molecular weight (HMW) molecule. The smallest HA is termed oligosaccharides (o-HA) (~ 400 to 20000 Da) and the HA with sizes between HMW and o-HA is termed low molecular weight (LMW). In the ECM, native HA is present as HMW molecule. In presence of an injury or an pathology such as cancer, HMW HA can be degraded in LMW HA and o-Ha [48]. HMW HA and its fragments influence differently the mechanisms involved in various biological behaviors of cancer cells. The size dependence of HA signaling still poor understood, but it may be related with the fact that different polymer sizes interact differently with the respective receptors and then induce differently the intracellular pathways [48, 49]. As an example, Yang and co-workers demonstrated that HMW HA and o-HA have distinct effects on CD44 receptor clustering [50]. HA with high number of repeated disaccharides has multivalent sites for CD44 binding, whereas o-HA has very few binding sites. Hence, HMW HA induced the clustering of CD44 receptor needed for the activation of intracellular signaling. In contrast, o-HA played as an antagonist reducing the activity of CD44 receptor and the promotion of intracellular signaling pathways [50]. This was also demonstrated by Misra *et al.*, where o-HA reduced the activation of PI3K and mitogen-activated protein kinases (MAPKs) pathways [18]. Additionally, with the inactivation of this pathways pro-apoptotic events occurred (*e.g.*, decreased phosphorylation of BAD and increased caspase-3 activity) and cancer cells sensitivity to chemotherapeutic drugs, such as Doxorubicin, increased [18]. In fact, Zeng *et al*. considered the possibility to treat tumors by using o-HA, since the administration of the molecules (3 to 12 disaccharide units) in B16F10 murine melanoma cells clearly reduced the growth of this cells [51].

Other study that demonstrated the influence of HA molecular weight in cancer cells behavior was performed by Afify *et al*. [52]. They showed that breast cancer cells (MDA-MB-468, MDA-MB-231, and MDA-MB-157) have higher invasiveness potential when cultured in presence of HMW HA, and cells cultured with o-HA led to the loss of invasion ability [52]. This inhibition of invasiveness was also found when cells were pre-incubated with anti-CD44 antibodies, demonstrating that o-HA act in similar way to the CD44 inhibitors.

1.2. Tumor spheroids assembly in HA-based structures

Cells form spheroids when they are grown in non-or poorly adhesive surfaces. In such conditions, cell-cell interactions are privileged and 3D cellular aggregates are obtained. Non-adhesive or poorly adhesive surfaces used for spheroids assembly include non-treated petri dishes/plates (*e.g.*, hydrophobic plates), traditional cell culture polystyrene surfaces covered with a layer of non-adhesive subtracts (*e.g.*, agar or agarose) [53], or even 3D structures (*e.g.*, scaffolds) produced with poorly adhesive biomaterials (*e.g.*, polydimethylsiloxane) [54]. However, these polymers do not interact with cancer cells receptors and are unable to

activate specific signaling pathways that can regulate tumor cells response to therapeutics, as occurs *in vivo*. In opposition, HA is a non-adhesive polymer that can regulate cancer cells behavior through cell-HA signaling. HA has been previously used for avoiding cellular adhesion by Chauzy *et al*. [55] and Stark *et al*. [56]. Their results revealed that various cell lines (Hep-G2 human hepatocellular carcinoma, PC-12 rat adrenal pheochromocytoma and CB109 human glioblastoma multiforme (GBM) cells) were able to form clusters when they were seeded on HA-coated surfaces [55, 56]. Additionally, Khademhosseini *et al*. also observed that bovine serum albumin, immunoglobulin and fibronectin displayed a lower adhesion to HA coated surfaces than to glass dishes [24]. Such result highlights the poor adherent properties of HA, since cell adhesion to biomaterials demands a prior protein adhesion to their surfaces [24-26].

Taking into account HA properties, different researchers started to apply this polymer for the production of 3D structures or as coating material for flat surfaces aimed for spheroids self-assembly [23, 38, 39, 47, 57, 58]. The HA structures investigated so far, include scaffolds, fibrous meshes, hydrogels, beads or HA coated polystyrene surfaces (Figure 4). Further details of these structures are presented in the following topics.

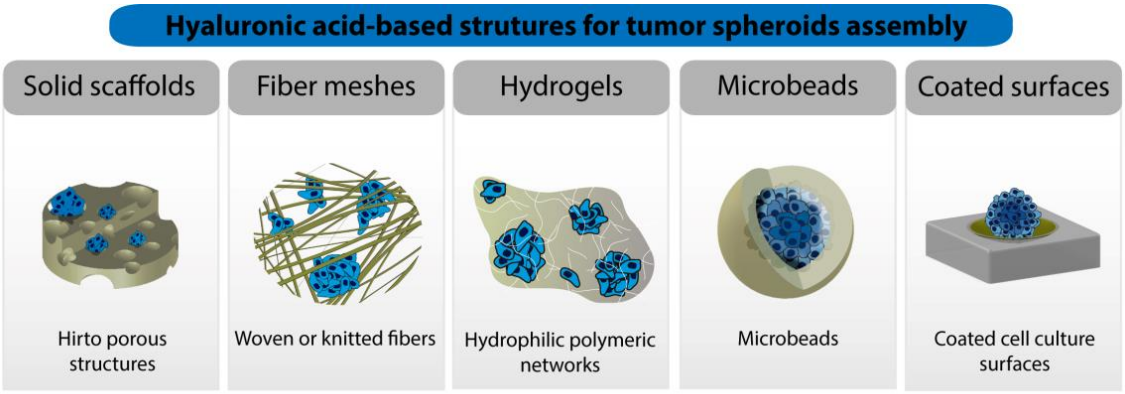

Figure 4. HA-based structures for tumor spheroids assembly: solid scaffolds, fiber meshes, hydrogels, microbeads and HA coated traditional cell culture surfaces.

1.2.1. Tumor spheroids assembly using HA composed hydrogels

Hydrogels are formed by hydrophilic polymeric networks that retain large amounts of water and exhibit tissue-like elastic properties (Figure 4) [59]. HA has been used for hydrogels production aimed for a wide range of medical applications (*e.g.*, cosmetic, skin regeneration) [60, 61].

Prestwich *et al*. produced an HA-based hydrogel by modification of HA with functionalized hydrazides for several applications, including drug delivery, biomolecules purification, and to study the role of HA in cellular adhesion and signaling [62]. Years later, David and co-workers used an adaptation of the method previously used by Prestwich to produce HA-based hydrogels with suitable properties for 3D cell culture [23, 47]. Those hydrogels were used to investigate the HA role in cancer pathogenesis and in anticancer drug sensitivity. In their

study, various cell lines migrated into the HA hydrogel, originating clusters and colonies of cells [23]. In another study from the same authors, it was demonstrated that various cancer cell lines (brain metastasis SA87, lung carcinoma (NCI-H460 and H460M)) have a higher capacity to avoid the apoptotic and anti-invasive effect of Doxorubicin and 5-fluorouracil, than the same cell lines cultured in 2D [47]. Such resistance may be promoted by the limited diffusion of drugs within hydrogels, similarly to what happens in real tumors, or as a consequence of CD44 and RHAMM receptors activation, which are involved in the activation of anti-apoptotic pathways [47].

Gurski *et al*. reported the use of HA-based hydrogels to formulate C4-2B bone metastatic prostate cancer spheroids that were used for anticancer drug screening purposes. In this study, camptothecin, docetaxel and rapamycin were used as model drugs [63]. Furthermore, these authors also used the produced hydrogels to characterize drug penetration and to predict their diffusion within hydrogel matrix [63]. To accomplish such objective, the hydrogel was incubated with hyaluronidase, which is responsible for HA degradation. Then, the amount of drug that remained in the matrix or was released to the surrounding media was determined by spectrofluorimetry and high-performance liquid chromatography [63].

Another interesting application of HA-hydrogels was reported by Xu and co-workers, that used these matrices for producing a 3D bilayer platform that supported the assembly of LNCaP prostate tumor spheroids [64]. This platform was composed of a mixture of HA functionalized with acrylate groups (HA-AC) and reactive thiols (HA-SH) that were covalently crosslinked [64]. The thioether bonds established between the sulfhydryl groups of HA-SH and the hydrazide amides of HA-AC make the hydrogel network very stable and increased its resistance to degradation, allowing cell culture for long periods, in contrast to unmodified-HA [64].

Pan *et al*. demonstrated that HA-based hydrogels can also be used to study the metastatic behavior of cancer cells [41]. These authors produced spheroids by seeding cells (786-O), isolated from bone metastases of patients with renal clear cell carcinoma (RCC), on a HA-hydrogel [41]. Then, they performed a real-time PCR analysis and fluorescence microscopic assays. The obtained results demonstrated that spheroids express higher levels of Cad11 and CXCR4 (that are involved in the mechanism of RCC bone metastasis), when in contact with HA [41]. Such data, allow them to propose that 3D HA-based hydrogels can be used for the assembly of spheroids aimed to be applied in drug screening for the treatment of bone metastatic RCC.

1.2.2. HA-based solid scaffolds used for tumor spheroids assembly

Porous scaffolds have been used for cell growth in 3D (as can be observed in Figure 4) [65]. The maintenance of scaffold' integrity during cell culture period is essential for conferring support and also for allowing nutrients, gases and waste exchange as well as ECM deposition.

As such, it is crucial that these solid structures present a slow degradation rate, appropriate swelling behavior and a suitable mechanical resistance. Although, scaffolds composed only by HA do not demonstrate such properties [66]. To produce HA-based scaffolds with the required properties, Florczyk *et al.* made a HA/chitosan blend where the negatively charged carboxyl groups (-COOH) of HA interacted with the positively charged amino groups ($-NH_2$) of chitosan and formed polyelectrolyte complexes (PEC) [38]. Then, these PEC were used for the production of porous scaffolds with a reduced swelling capacity and an increased stability [38]. U-118 MG GBM spheroids were formed using these scaffolds. Over 15 days, scaffolds showed a limited swelling and no significant degradation or shape variation was noticed [38]. Authors also reported that spheroids interaction with the HA resulted in the overexpression of CD44 and other stem cell markers (nestin, musashi-1, glial fibrillary acidic protein (GFAP) and hypoxia-inducible factor 1-alpha (HIF-1α)) [38]. Such results clearly demonstrate that GBM spheroids self-assembled in HA-based scaffolds display a gene expression profile similar to that found in GBM tumors. Furthermore, cells from GBM spheroids also displayed a higher proliferation, invasive capacity and resistance to Doxorubicin and Temozolomide [38]. These data emphasize the suitability of HA-based scaffolds to assemble spheroids with a structural arrangement that reproduce glioblastoma multiform tumor features.

1.2.3. HA-based fiber meshes as possible supports for tumor spheroids assembly

HA was also used for the production of electrospun fibrous meshes. These meshes are formed by individual fibers, either woven or knitted, that display a 3D architecture similar to that found in the ECM (Figure 4) [67]. In addition, due to the high solubility of HA in water, it is recognized for being more cell friendly than other polymers, like polycaprolactone (PCL), that are only soluble in organic solvents. Such solvents usually have some degree of toxicity for cells. Nonetheless, HA solution viscosity may be a drawback for fibers production, since during the electrospinning process, viscous solutions travel as a jet to the collector of the electrospinning device, leading to the formation of polymeric clusters. Additionally, due to the high ability of HA to retain water, there is a tendency to occur fibers fusion. To overcome such shortcomings, temperature, HA solution concentration, HA molecular weight and HA solubilization in other solvents (*e.g.*, ethanol) has been assayed [68]. Optionally, HA fibers can also be produced by using an warm air blowing system engaged on the electrospinning apparatus, a process also known as electroblowing [68]. Such modification allowed a faster and better water evaporation, that is crucial for the formation of uniform fibers without HA beads [68]. Nevertheless, as previously described for porous solid scaffolds, the stability of fibers only composed of HA is very limited. To increase their stability hyaluronan cross-linking has already been tested (reviewed in [61]). Still, HA fibers steadiness can be further improved by blending HA with other polymers. Li *et al.* electrospun HA emulsified with other polymers, namely silk fibroin (SF) and PCL, and by performing mechanical and degradation tests they

observed that PCL/SF/HA fibers demonstrated high tensile strength and maintained their integrity over 7 days when incubated in a saline solution [26].

Hitherto, HA-based fibers applicability for spheroids assembly still poor investigated since the ability of HA-based fibers to grow cellular aggregates was only demonstrated by Kim and co-workers, that applied methacrylated HA (MeHA) and cysteine-containing RGD peptides to produce fibers by electrospinning [69]. The fibers were used to culture human mesenchymal stem cells (MSCs) for cartilage repair strategies. MSCs cells formed cellular aggregates after long periods of culture and express chondrogenic markers (*e.g.*, aggrecan and Sox 9)[69].

1.2.4. HA microbeads used for cells encapsulation and tumor spheroids assembly

Another strategy used for spheroids assembly involves cell encapsulation or immobilization within microbeads or shells [70]. Up to now, Alginate is the most used biomaterial for cell encapsulation intended for tissue engineering applications or 3D cell culture. Recently, microbeads of HA were also produced for the same purpose (Figure 4). Initially, HA-hydrogel beads were used to encapsulate chondrocytes, using a microinjection technique, in order to allow the regeneration of defective cartilage tissues [71]. In 2010, Skardal and co-workers studied the applicability of HA for the production of beads that could be used for the production of 3D tumor tissue models [72]. To accomplish that, porous microbeads (Sephadex® G-50 beads (GE Healthcare Biosciences)) were impregnated with a hyaluronan-based semi-synthetic matrix solution composed by thiol-modified gelatin and thiol-modified hyaluronan (Extracel™ (Glycosan Biosystems) [72]. After the formation of the HA coated beads, cells and beads were maintained in a rotating wall vessel system to allow the assembly of 3D Int-407 (a HeLa derivative cell line) cell culture [72]. This approach maintains cells in suspension, favoring cells attachment to the beads surface and also their migration and aggregation within the bead [72]. Subsequently, authors compared the morphology of 3D cell culture formed in the HA-based microbeads with those obtained using collagen-coated Cytodex® beads (GE Healthcare Biosciences). The gathered results demonstrated that Int-407 cultured in 3D HA-based beads mimics more accurately the structural arrangement displayed by real tumors, than those cultured in collagen-based beads [72].

1.2.5. Tumor spheroids assembly in cell culture plates coated with HA

The first study reporting spheroids assembly on HA coated surfaces (Figure 4) was performed by Huang *et al.* [73]. These researchers coated petri dishes with a mixture of chitosan-HA and then seeded stem cells (MSCs) on it to form spheroids [73]. Such spheroids displayed a size-dependent behavior on HA/chitosan ratios, *i.e.,* larger spheroids were obtained for higher biomaterials ratios [73].

Hsu and Huang [74] further optimized the coating procedure of cell cultures plates. They used ethyl (dimethylaminopropyl) carbodiimide/N-hydroxysuccinimide (EDC/NHS) coupling

chemistry to perform the cross-linking between the amino groups of chitosan and the carboxylic groups of HA, strengthening the HA interaction with chitosan. The coated surfaces were then used to produce A549 and H1299 non-small-cell lung tumor spheroids [39]. Then, spheroids diameters measurements confirmed the reproducibility of the method and, as previously reported, higher amounts of HA led to the formation of bigger A549 and H1299 spheroids [39]. However, the main achievement of this study was the acquisition of stem-like properties and epithelial-mesenchymal transition (EMT) markers (Nanog, Sox2, CD44, CD133, N-cadherin, and Vimentin) by non-stem cancer cells that were cultured in cell culture plates coated with HA [39]. In addition, A549 and H1299 spheroids demonstrated higher motility and invasive and multidrug resistance (5-6 times more resistant to Cisplatin and 16-56 times to Methotrexate), as a consequence of the upregulation of ECM degradation enzymes (MMP2 and MMP9), anti-apoptosis genes (baculoviral inhibitor of apoptosis repeat-containing 5 (BCRC5) and Bcl-2), MRD1 and drug efflux pumps (ATP-binding cassette sub-family G member 2 (ABCG2)) [39]. Huang and co-worker suggested that these results were obtained due to the interactions between the CD44 and the HA, since the higher amounts of HA leaded higher expression of stemness and cancer stem cell (CSC) markers [39].

More recently, Lai and Tu [58] tested the effect of coating cell culture plates with HA of different molecular weights (35, 360 and 1500 kDa) for producing reproducible spheroids of rabbit corneal keratocytes [58]. The produced spheroids demonstrated similar gene expression profile to that of cells grown *in vivo*. More specifically, spheroids demonstrated upregulated gene expression of keratinocytes markers, like keratocan and lumican [58]. More important, authors tested how HA molecular weight affect surface properties (charge, topography and hydrophilicity) and spheroids formation. Spheroids were bigger and more easily formed when cells were placed on 1500 kDa HA coated surfaces, where the surface charge was more negative, more roughened and less hydrophobic [58]. In the surfaces coated with HA with lower molecular weights, occurred more cellular spreading and cellular attachment to the surface. In fact, for HA with the lowest molecular weight, spheroids assemble did not occurred [58].

1.3. Aims

The main aim of this thesis was the optimization of heterotypic breast cancer 3D spheroid models for future development and investigation of new anticancer therapeutics and drug delivery systems.

The specific aims of this thesis include:

- Development of spheroids that mimic *in vitro* the heterogenic cellular constitution of breast tumor by using malignant breast cells and stromal fibroblasts;
- Production and optimization of heterotypic breast cancer spheroids models in surfaces coated with HA;
- Evaluation of the HA concentration and of the initial cell-seeding density influence on size, shape and number of spheroids formed;
- Analysis of the structural features of 3D tumor spheroids and its ability to reproduce the main features of breast tumors.

Chapter II

Materials and Methods

2. Materials and Methods

2.1. Materials

Oestrogen-dependent human breast adenocarcinoma (MCF-7) cells were acquired from ATCC (Middlesex,UK). Normal Human Dermal Fibroblasts (NHDF) were bought from PromoCell (Labclinics, S.A.; Barcelona, Spain). Cell culture plates and T-Flasks were obtained from Thermo Fisher Scientific (Porto, Portugal). Sodium hyaluronate (HA) (1500 to 2200 kDa) was purchased from Acros Organics (New Jersey, USA). Acridine orange base (AO), cacodylate, Dulbecco's Modified Eagles's Medium F-12 (DMEM-F12), ethanol, glutaraldehyde, paraformaldehyde (PFA), phosphate-buffered saline solution (PBS), trypsin and ethylenediaminetetraacetate (EDTA) were got from Sigma-Aldrich (Sintra, Portugal). Cell imaging plates were acquired from Ibidi GmbH (Munich, Germany). Propidium Iodide (PI) was purchased from Invitrogen (Carlsbad, CA, USA). Fetal bovine serum (FBS) was obtained from Biochrom AG (Berlin, Germany).

2.2. Preparation of hyaluronic acid-coated 96-well plates

96-well cell culture plates were coated with 200 µL of HA solution with different concentrations (ranging from 1.0 to 5.0 mg/mL). Then, HA-coated plates were dried by maintaining them at 37°C during 3-4 days. Subsequently, cell culture plates were sterilized by ultraviolet (UV) irradiation for 30 min. A scheme of the procedure used for the preparation of HA-coated cell culture plates is present in Figure 5.

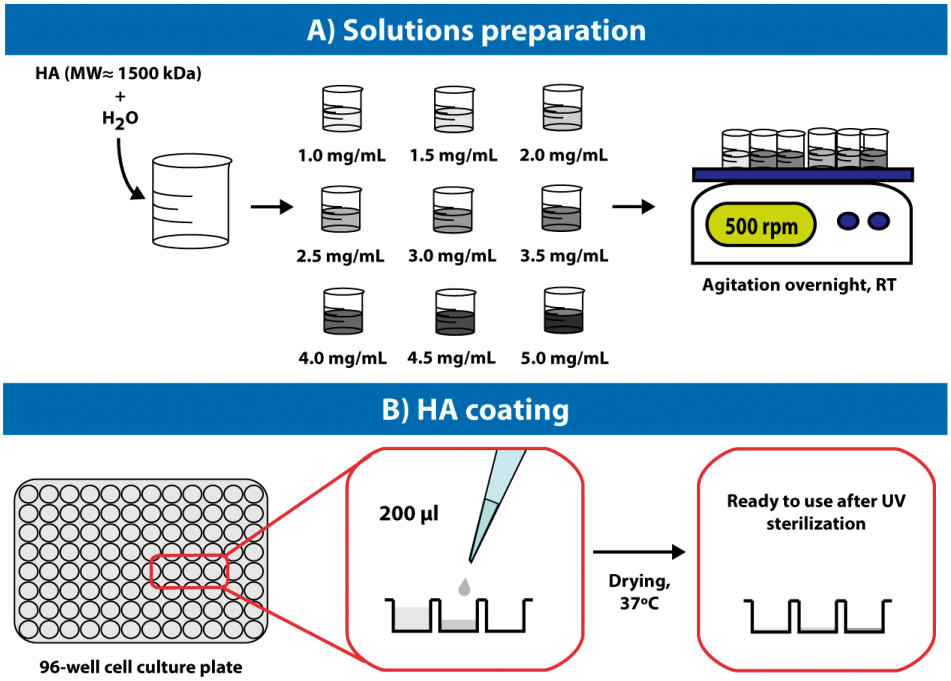

Figure 5. Preparation of the 96-well cell culture plates coated with HA aqueous solutions. HA concentrations ranging from 1.0 to 5.0 mg/mL.

2.3. Production of homotypic and heterotypic breast cancer spheroids

MCF-7 and NHDF cell lines were grown in DMEM-F12 medium supplemented with 10% FBS, 1% streptomycin and gentamycin in 75 cm^2 T-flasks with a humidified atmosphere of 5% CO_2, at 37°C [10]. Initially, to determine the influence of HA concentration on spheroids assembly, homotypic NHDF and heterotypic MCF-7:NHDF spheroids were assembled by seeding cells onto 96-well plates pre-coated with HA solutions at different concentrations (ranging from 1.0 to 5.0 mg/mL). After, to investigate the influence of the initial cell-seeding density on NHDF and MCF-7:NHDF spheroids formation, cells were seeded at various densities (25000, 50000 and 100000 cells/well) onto 96-well plates pre-coated with different HA solutions. Furthermore, the heterotypic spheroids were assembled, in this study, using two different ratios of cancer to fibroblast cells (3:1 and 1:1). These different cancer cells to fibroblasts ratios were selected in order for a more realistic model of breast tumors be obtained [75, 76].

2.4. Characterization of the size and morphology of spheroids by optical microscopy

Spheroids assembly, growth and morphology were visualized using an Olympus CX41 inverted optical microscope equipped with an Olympus SP-500 UZ digital camera at different time points. The obtained images were analyzed with an image analysis software - ImageJ, National Institutes of Health [77], using a method previously described by Costa *et al.* [10]. Five independent spheroids, produced with the same experimental setup, were used for size and morphology evaluations.

2.5. Characterization of spheroids' surface morphology by scanning electron microscopy analysis

For scanning electron microscopy (SEM) analysis, spheroids samples were prepared as previously described [10]. In brief, spheroids were collected and washed with cacodylate buffer 0.1 M (PBS 1% (w/v)) for 1h at room temperature (RT). After, samples were washed with PBS and then fixed using 2.5% glutaraldehyde in PBS at RT, for 2 h. Subsequently, samples were dehydrated in graded ethanol solutions (50%, 60%, 70%, 80%, 90% and 100%) and then left at RT overnight to completely dry. Prior to visualization, spheroids were sputter-coated with gold and then visualized using a Hitachi S-3400N (Tokyo, Japan) electron microscope operated at an accelerating voltage of 20 kV and at several magnifications.

2.6. Characterization of spheroids' structure by confocal laser scanning microscopy analysis

Cell distribution within spheroids was studied by using a fluorescence-based live/dead assay. In brief, spheroids were labeled with PI (10 μg/mL) during 90 min. Then, they were washed with PBS and chemically fixed by PFA 4% (w/v) overnight, at 4°C. Subsequently, spheroids were incubated with AO for 2 h and then rinsed with PBS. Finally, spheroids were visualized using a Zeiss LSM 710 laser scanning confocal microscope (Carl Zeiss SMT, Inc., Oberkochen, Germany) and image analysis was performed with a Zeiss Zen software (2011).

2.7. Statistical analysis

The statistical analysis of the obtained results was performed by using one-way ANOVA with Newman–Keuls multiple comparison test. A *P* value lower than 0.05 (*$P < 0.05$) was considered statistically significant. Data analysis was performed in GraphPad Prism v6.0 (Trial version, GraphPad Software, CA, USA).

Chapter III

Results and Discussion

3. Results and Discussion

Breast cancer microenvironment is composed of cancer and stromal cells, such as fibroblasts, endothelial, immune system and adipocytes cells [78]. Among the stromal cells, fibroblasts have a pivotal role in cancer progression and resistance to anticancer treatments [79, 80]. Fibroblasts are able to interact with other cells present in the tumor mass and secret hepatocyte, fibroblast, epithelial and insulin-like growth factors that are involved in proliferation of cancer cells and activation of mechanisms that contribute to apoptosis resistance [76, 80, 81]. In a study performed by Martinez-Outschoorn *et al.*, the influence of fibroblasts on cancer cells response to pharmaceutical compounds was highlighted since 2D co-cultures of MCF-7:fibroblasts displayed a higher resistance to Tamoxifen than to the homotypic 2D cultures composed of MCF-7 cells [82]. Sabhachandani *et al.* also reported that spheroids composed of MCF-7 and fibroblasts had a higher survival rate to Doxorubicin than MCF-7 spheroids [83].

Herein, heterotypic breast cancer spheroids were assembled for the first time on HA-coated surfaces to better represent the breast tumors 3D organization and cells-ECM interactions. To accomplish that, in the first stage of this study HA-coated surfaces were used to assemble NHDF spheroids, according to the method previously described by Lai and Tu [58]. NHDF cells were seeded on HA (molecular weight≈ 1500 kDa) coated surfaces (1.0 mg/mL). The optical microscopic images present in Figure 6, demonstrate that NHDF cells aggregated and formed spheroids after 1 day of culture and then were grown for 7 days.

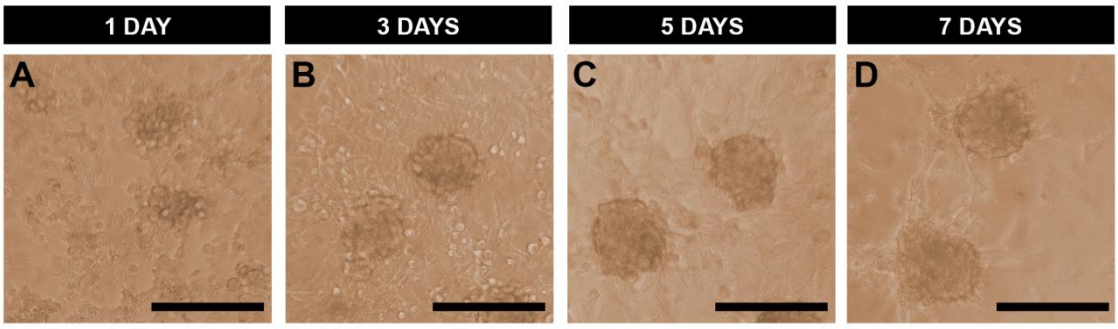

Figure 6. Optical contrast microscopic images of NHDF spheroids that were produced on surfaces coated with 200 µL of HA (1.0 mg/mL) and by using an initial cell-seeding density of 25000 cells/well, during 7 days of culture (A-D). Scale bar corresponds to 200 µm.

Still, these NHDF spheroids had small diameters (≈ 200 µm) and therefore these cellular aggregates may not properly represent the conditions found in solid tumors, since in literature, it has been described that spheroids with a diameter larger than 500 µm are those that better mimic the features of solid tumors. Spheroids with this size become more compact and compartmentalized, forming pH, nutrient, and waste removal gradients, as well as display an anticancer therapeutics resistance profile similar to that found *in vivo* [84-87].

Hereafter, different HA concentrations and various initial cell-seeding numbers per well were used to investigate the optimal conditions for gathering spheroids with suitable properties for drug screening purposes.

3.1. Evaluation of the effect of HA concentration and the initial cell-seeding density on spheroids size

In a previous study Huang *et al*. demonstrated that by increasing the HA concentration used for coating surfaces (which are used for spheroids assembly) can promote the formation of larger cellular aggregates [39]. Their results showed that tumor spheroids composed of human non-small cell lung cancer (A549 and H1299 cells) and assembled on chitosan-HA surfaces displayed a larger size when cells were seeded on surfaces with higher HA:chitosan ratios [39]. Accordantly, in order to obtain NHDF homotypic and MCF-7:NHDF heterotypic spheroids with larger diameters, cells were seeded on 96-well plates covered with higher concentrations of HA (> 1.0 mg/mL). Figure 7 A-C show different spheroids that were assembled on surfaces coated with different concentrations of HA (1.0, 1.5, 2.0, 2.5, 3.0, 3.5, 4.0, 4.5 and 5.0 mg/mL) in which were initially seeded 25000 cells/well.

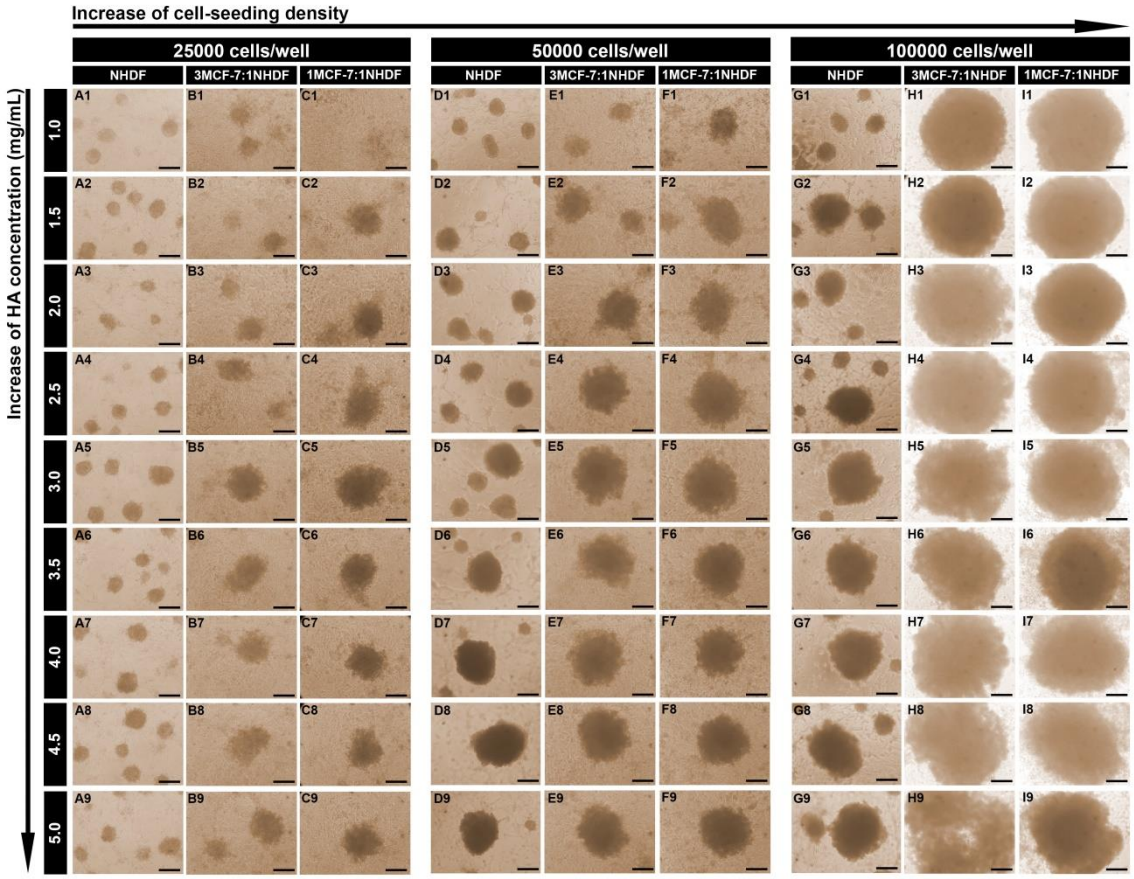

Figure 7. Optical contrast microscopic images of NHDF, 3MCF-7:1NHDF and 1MCF-7:1NHDF spheroids after 5 days of cells being seeded. Spheroids were formed in 96-well plates coated with 200 µL of HA solutions (1.0, 1.5, 2.0, 2.5, 3.0, 3.5, 4.0, 4.5 and 5.0 mg/mL). For each HA concentration, various initial cell-seeding densities (25000 (A-C), 50000 (D-F) and 100000 (G-I) cells/well) were tested. Scale bar corresponds to 200 µm.

Through the analysis of Figure 8 A-C, it was possible to observe that the influence of the HA concentration on spheroids size was not significant when 25000 cells/well were used for NHDF spheroids production. In fact, the NHDF spheroids formed by seeding 25000 cells per well, reached approximately 200 µm after 7 days of culture, independently of the HA concentration used (Figure 8 A).

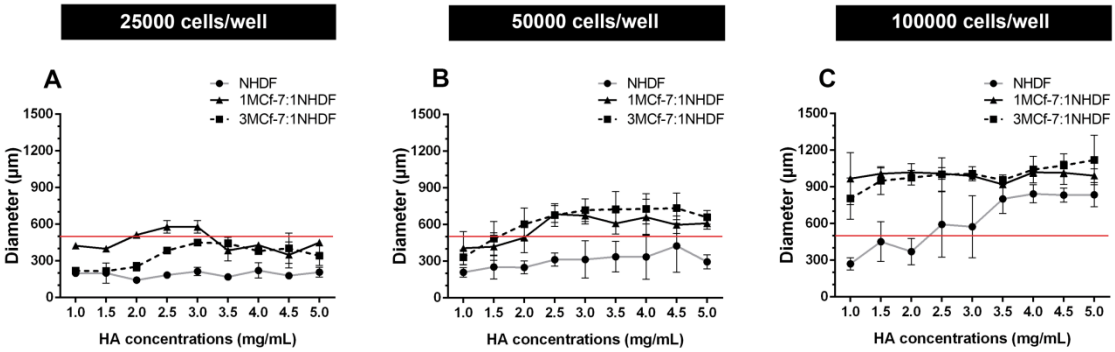

Figure 8. NHDF, 3MCF-7:1NHDF and 1MCF-7:1NHDF spheroids diameter after 7 days of cells being seeded on 96-well plates coated with 200 µL of HA solutions with different concentrations (1.0, 1.5, 2.0, 2.5, 3.0, 3.5, 4.0, 4.5 and 5.0 mg/mL). Different initial cell-seeding numbers (25000 (A), 50000 (B) and 100000 (C)) were used. *P<0.05.

Moreover, we also noticed that heterotypic spheroids, produced with an initial cell number of 25000 cells/well, were only consistently assembled when HA concentrations higher than 3.5 mg/mL were used. Additionally, MCF-7:NHDF spheroids diameters did not surpass the 500 µm even for the higher HA concentrations (Figure 8 A).

Therefore, to improve spheroids formation and also to get spheroids with higher diameters, the initial cell-seeding density was increased by taking into account a study of Ma *et al.* [88]. In their work, the size of HeLa cervical cancer spheroids formed on agarose coated surfaces revealed to be dependent on the initial cell number used for spheroids assembly, *i.e.*, bigger spheroids are obtained when a higher number of cells is initially seeded on wells [88].

In Figure 7 and 8, it is possible to observe the influence of the initial cell-seeding number (25000, 50000 and 100000) on NHDF and MCF-7:NHDF spheroids size. In general, the increase of the initial number of cells seeded (50000 and 100000 cells/well) led to the formation of spheroids with larger diameters (Figure 8). NHDF spheroids attained diameters of 200–1000 µm, whereas MCF-7:NHDF spheroids reached diameters in a range of 300–1200 µm (Figure 8 B and C). Moreover, spheroids produced with a 3MCF-7:1NHDF ratio were slightly bigger than those produced with 1MCF-7:1NHDF ratio, since spheroids produced with a higher number of MCF-7 cells, tend to be less cohesive, especially when 100000 cells/well were used (Figure 7). Such result is in agreement with our previous study, where spheroids with a higher number of MCF-7 than NHDF cells were less compact, and therefore presented a larger diameter [10].

Additionally, despite the influence of the HA concentration on spheroids size was not significant when 25000 cells/well were used for spheroids production, when a higher number of cells were initially seeded per well, it was possible to observe that the HA concentration can influence the spheroids size, as previously described by Huang *et al*. [39]. After 7 days of culture, the homotypic and heterotypic spheroids displayed diameters higher than 500 µm when 50000 and 100000 cells were seeded on surfaces coated with HA solutions at concentrations higher than 2.5 mg/mL (Figure 8 B and C).

3.2. Characterization of the effect of the initial cell-seeding density and of the HA concentration on spheroids shape

The spherical morphology of the cellular aggregates is the most appropriate when these microtissues are aimed for therapeutics testing. Such morphology gives to the 3D cellular aggregate a homogeneous pH, gases and nutrients distribution, as well as cellular density. Furthermore, in the spherical spheroids the therapeutics are equally distributed through the surface, *i.e.*, therapeutics are all at the same distance from the center of the spheroids [5].

Therefore, all the acquired optical microscopic images were analysed by using ImageJ software [77], as illustrated in Figure 9. The spheroids major and minor axis were measured to determine the sphericity of 3D cellular aggregates trough the calculation of spheroids asymmetry, using Equation (1) as previously described by Cheng and co-workers [89]. Spheroids are more symmetric and spherical when their shape asymmetry is approximately equal to 1 (Figure 9).

$$\textbf{Spheroids asymmetry} = \frac{\text{Major Axis}}{\text{Minor Axis}} \qquad \textbf{(1)}$$

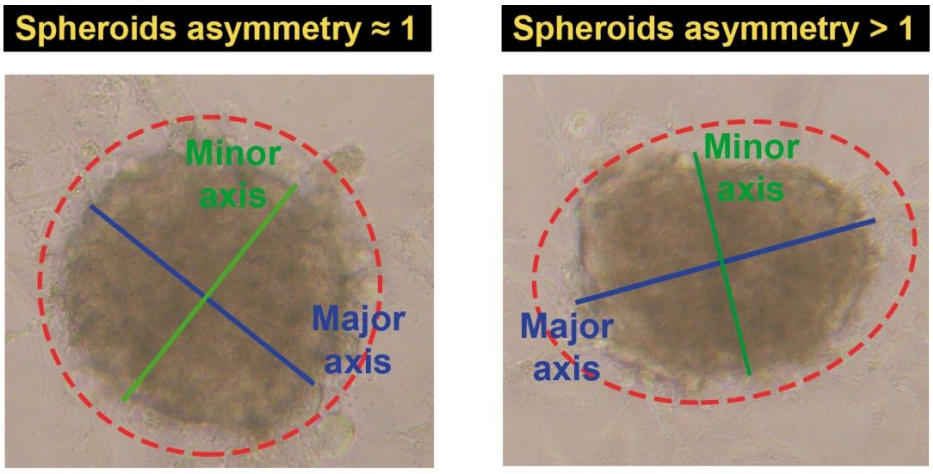

Figure 9. Determination of spheroids asymmetry. The size of spheroids major and minor axis was determined by ImageJ in order to calculate spheroids asymmetry. Spheroids with asymmetry values equal to 1.00 display a perfect spherical shape while spheroids with asymmetry values over 1 are considered less spherical.

Based on the obtained results, it was possible to conclude that NHDF, 3MCF-7:1NHDF and 1MCF-7:1NHDF spheroids shape is not significantly influenced by the HA concentration used for 96-well plates coating (Figure 10). In Figure 10 it was also possible to verify that when an initial higher cellular density was used, spherical-like cellular aggregates were obtained after 7 days of culture. Accordantly, the homotypic and heterotypic spheroids produced with 100000 cells/well demonstrate the lowest shape asymmetry. Additionally, in these conditions spheroids were assembled in a reproducible manner, which is crucial to obtain spheroids for drug high throughput screening [5, 90].

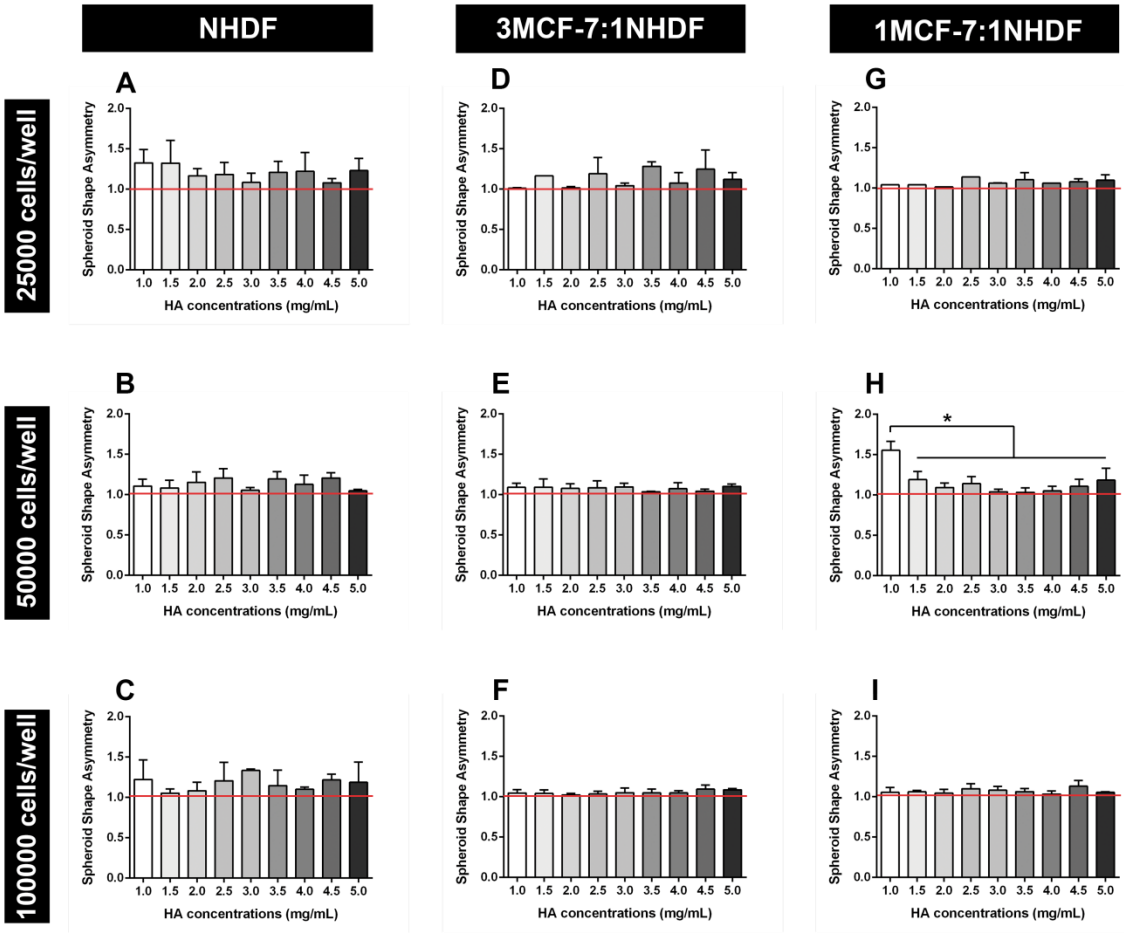

Figure 10. Influence of the HA concentration and initial cell-seeding density on NHDF (A-C), 3MCF-7:1NHDF (D-F) and 1MCF-7:1NHDF (G-I) spheroids asymmetry after 7 days of cells being seeded on 96-well plates coated with 200 µL of HA solutions (1.0, 1.5, 2.0, 2.5, 3.0, 3.5, 4.0, 4.5 and 5.0 mg/mL), using various initial cell-seeding numbers (25000, 50000 and 100000 cells/well). *P<0.05.

3.3. Evaluation of the effect of HA concentration and initial cell-seeding density on the number of spheroids formed

For therapeutic screening purposes, the individual cultivation of each spheroid is crucial, since it allows the imaging and the analysis of the response of each spheroid to the presence of drugs (*e.g.*, apoptosis and gene expression) [91, 92].

Therefore, we also evaluated the effect of the initial cellular density used and of the HA concentration (1.0 to 5.0 mg/mL) in the number of NDFH and MCF-7:NHDF spheroids formed per well (Figure 11).

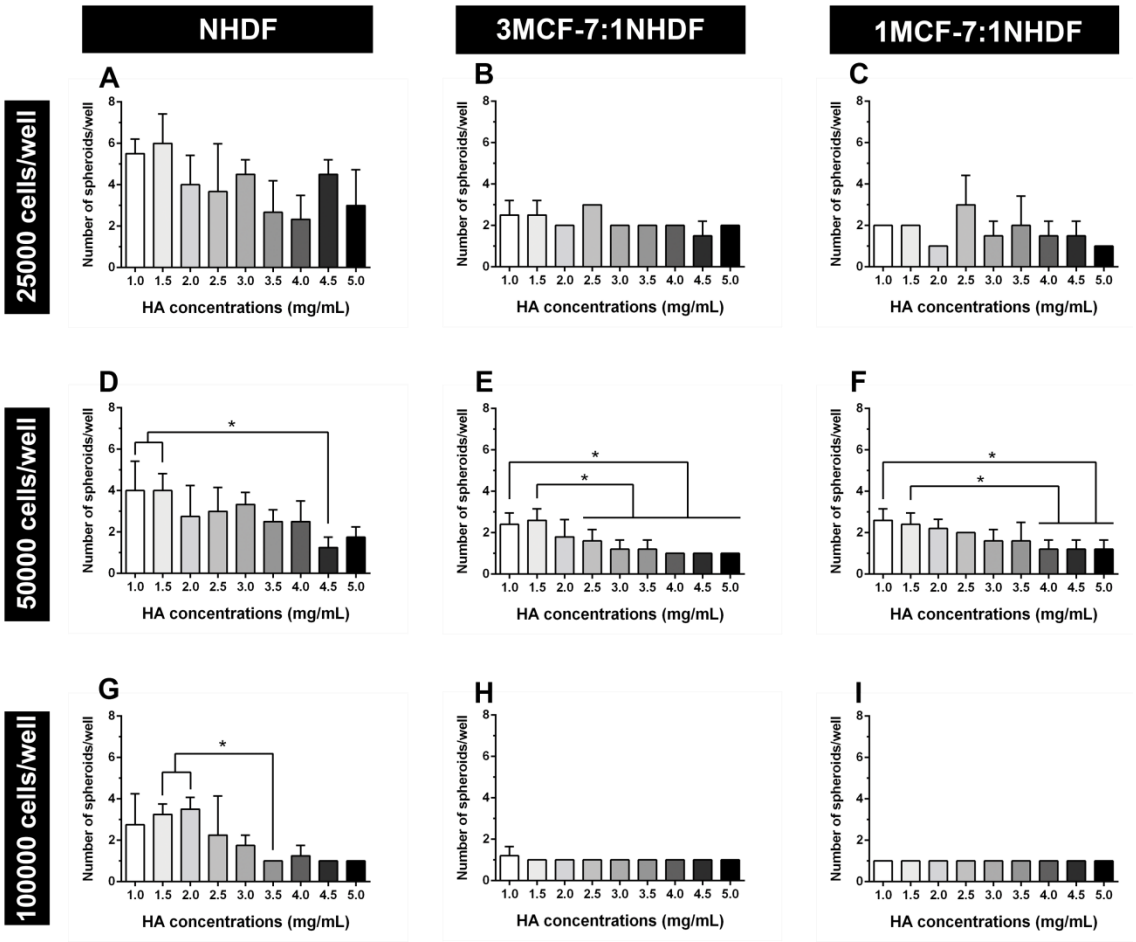

Figure 11. Number of NHDF, 3MCF-7:1NHDF and 1MCF-7:1NHDF spheroids produced per well when cells were seeded on 96-well plates coated with 200 µL of HA solutions (1.0, 1.5, 2.0, 2.5, 3.0, 3.5, 4.0, 4.5 and 5.0 mg/mL), using various initial cell-seeding densities (25000 (A-C), 50000 (D-F) and 100000 cells/well (G-I)). *P<0.05.

Through the analysis of the Figure 11 A-C it was possible to observe that when 25000 cells/well were seeded on HA-coated surfaces various homotypic and heterotypic spheroids were assembled per well. However, when the initial cell-seeding number was increased to 50000 and 100000 cells/well, the number of spheroids formed per well decreased (Figure 11 D-I). In fact, when 100000 cells/well were seeded only a single heterotypic spheroid was formed per well, independently of the HA concentration used (Figure 11 H and I, Figure 12). The same result was obtained for NHDF spheroids, when 100000 cells/well were initially seeded and a HA concentrations higher than 3.5 mg/mL were used (Figure 11 G).

A single spheroid is more easily obtained when cells are in co-culture and seeded on surfaces with higher concentrations of HA (Figure 12), since the cancer cells-fibroblasts and cell-HA interactions stimulate cells migration [33, 93], which is essential for the formation of a single spheroid [94].

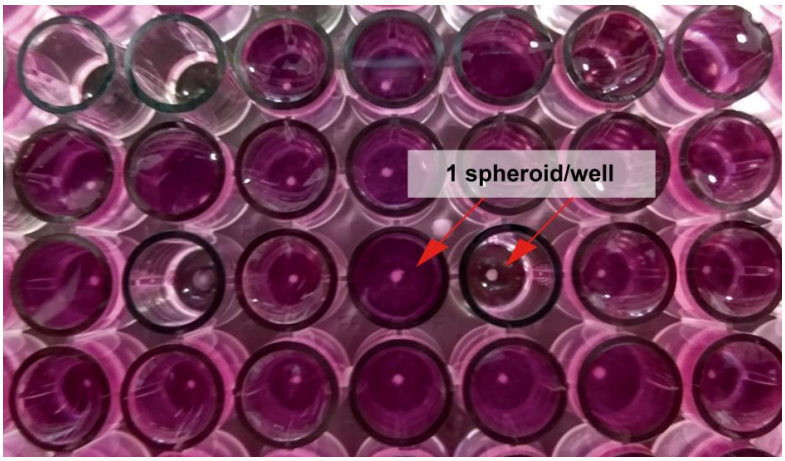

Figure 12. Macroscopic image of 3MCF-7:1NHDF spheroids produced by seeding 100000 cells/well on 96-well plates coated with 200 µL of HA (5.0 mg/mL), after 7 days of culture.

3.4. Characterization of the influence of horizontal stirring on spheroids formation

In a previous study, it was demonstrated that the stirring of the cell cultures can promote cellular aggregation and spheroids formation when cells are seeded on agarose concave surfaces [10]. The stirring promotes a closer physical contact between cells that leads to the formation of more cohesive and spherical spheroids [10, 91, 95]. Nonetheless, the effect of agitation on spheroids assembly when cells are seeded on HA-coated surfaces is still undisclosed. In this work, we evaluated the effect of using a 200 RPM horizontal stirring on NHDF spheroids production, by maintaining cells under stirring overnight at 37°C in a humidified atmosphere with 5% CO_2.

The obtained results are presented in Figure 13 and in contrast with the results previously reported for HNDF cells seeded on agarose and subjected to stirring [10], herein the agitation of NHDF cells did not promoted cells agglomeration when they are seeded on HA-surfaces. Even up to 5 days after cells being seeded, spheroids were not formed. Apparently, the stirring may have reduced the cells-HA interactions that are essential for the spheroids formation, as previously reported [39].

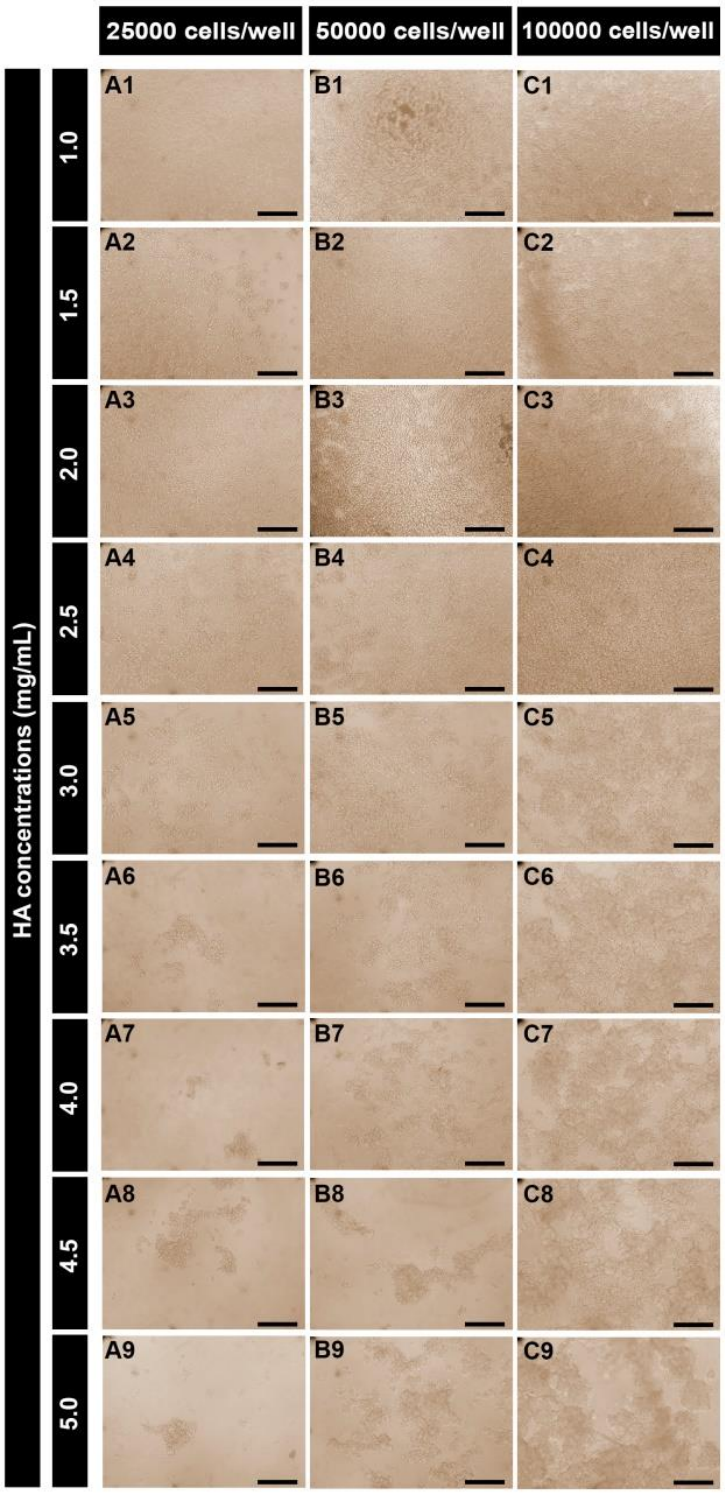

Figure 13. Optical contrast microscopic images of NHDF spheroids after 5 days of cells being seeded on 96-well plates coated with 200 µL of HA solutions with various concentrations (1.0, 1.5, 2.0, 2.5, 3.0, 3.5, 4.0, 4.5 and 5.0 mg/mL). For each HA concentration, various cell-seeding densities (25000 (A), 50000 (B) and 100000 (C) cells/well) were tested. After cells being seeded, plates were subjected to a 200 RPM horizontal stirring overnight. Scale bar corresponds to 200 µm.

3.5. Characterization of spheroids morphology

Cell-cell physical interactions play an essential role on spheroids integrity and intercellular signaling. This closeness between cells allows paracrine inter-cellular signaling, which has a

great influence on cells morphology, metabolism and proliferation under *in vitro* or *in vivo* conditions [5, 10].

As can be observed in Figure 14 A, 1MCF-7:1NHDF spheroids are organized in a 3D spherical structure and cell-cell physical interactions (*e.g.*, E-cadherins [10]) are established between both types of cells (arrows in Figure 14 B1, B2). In fact, it is possible to observe the presence of direct tight connections between cells due to the long filopodia protrusions, as previously reported in literature [10, 88].

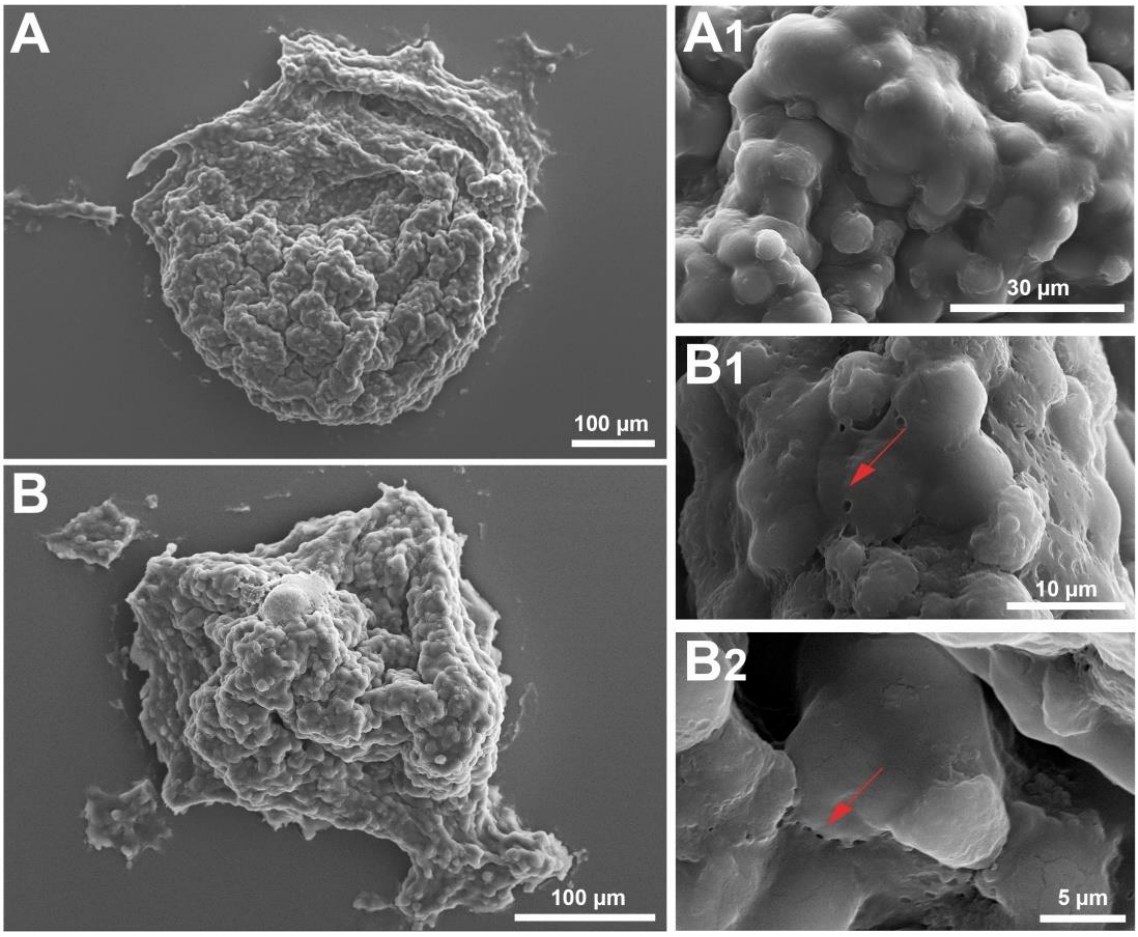

Figure 14. SEM images of 1MCF-7:1NHDF spheroids after 7 days of cells (100000 cells/well) being seeded on 96-well plates coated with HA solution (1.5 mg/mL) (A) and of 1MCF-7:1NHDF spheroid after 7 days of cells (50000 cells/well) being seeded on 96-well plates coated with HA solution (2.0 mg/mL) (B). Arrows indicate the cell-cell physical interactions.

3.6. Characterization of spheroids inner structure

Human solid tumors, due to their internal features, are characterized by a limited mass transport which is one of the main causes of tumors resistance to anticancer therapies. Such effect can be explained by the barrier formed by the cell-cell interactions that can be observed in the SEM images (Figure 14), but also by the increased cellular density in the center of spheroid (Figure 7) [96]. To further characterize cell density within 3MCF-7:1NHDF spheroids optical images were collected and then analyzed through ImageJ in order to

distinguish the regions within the spheroids with high cellular density (evidenced in red in Figure 15) from those with a lower cellular density [97].

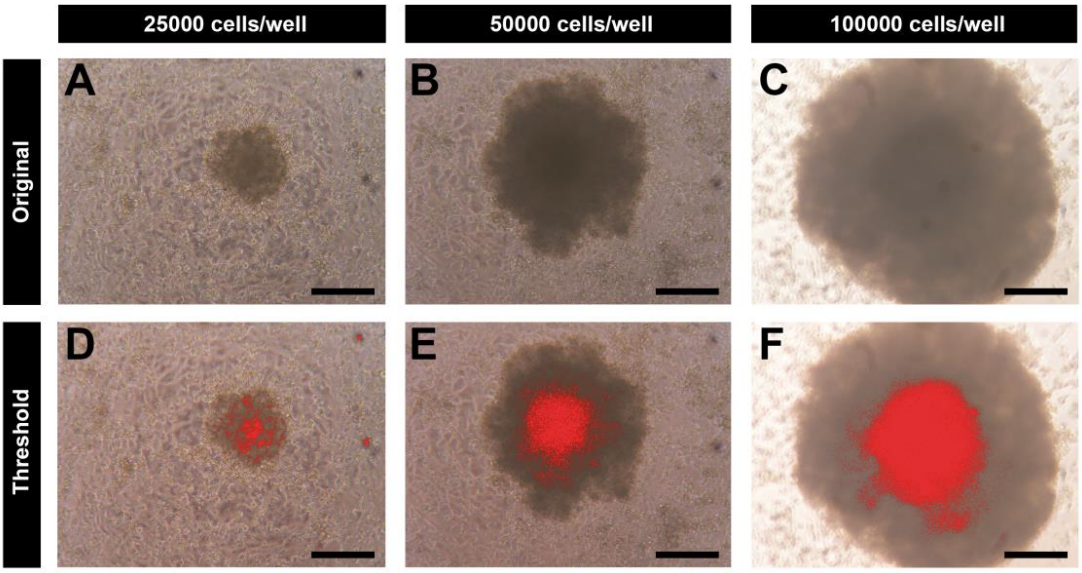

Figure 15. Optical contrast microscopic images of spheroids (A, B and C) produced with a different initial cell number (25000, 50000 and 100000 cells/well) that were seeded on 96-well plates coated with HA solution (4.0 mg/mL) and respective threshold images (D, E and F). Red regions represent the dense cellular regions of the spheroids.

Through the analysis of Figure 15 D it was possible to notice that spheroids assembled with 25000 cells/well present small regions of high cellular density distributed within the spheroid. In contrast, when a higher number of cells was used (50000 and 100000 cells/well) spheroids core had an increased cellular density (Figure 15 E and F), similarly to that found in the core of *in vivo* solid tumors [84, 98]. Wrzesinski and Fey [99] and Gong *et al*. [100] previously demonstrate that only spheroids with diameters higher than 300-400 μm have a dense and compact core.

Due to the high cellular density presented by larger spheroids, nutrients and gases exchange is also restricted within spheroid core leading to the formation of a hypoxic region, where necrotic cells emerge [101]. These cells express hypoxic growth factor [102], that can help the proliferation and survival of cancer cells in response to anticancer treatments [7]. To further characterize necrotic cells distribution within spheroids, a live/dead fluorescent based assay was performed (see Figure 16 for further details). This assay was only performed with the 3MCF-7:1NHDF spheroids produced by using 100000 cells/well (as initial cell seeding density), since the previous obtained results demonstrate that these spheroids gather all the conditions needed for drug screening, namely size, shape, sphericity and cellular density.

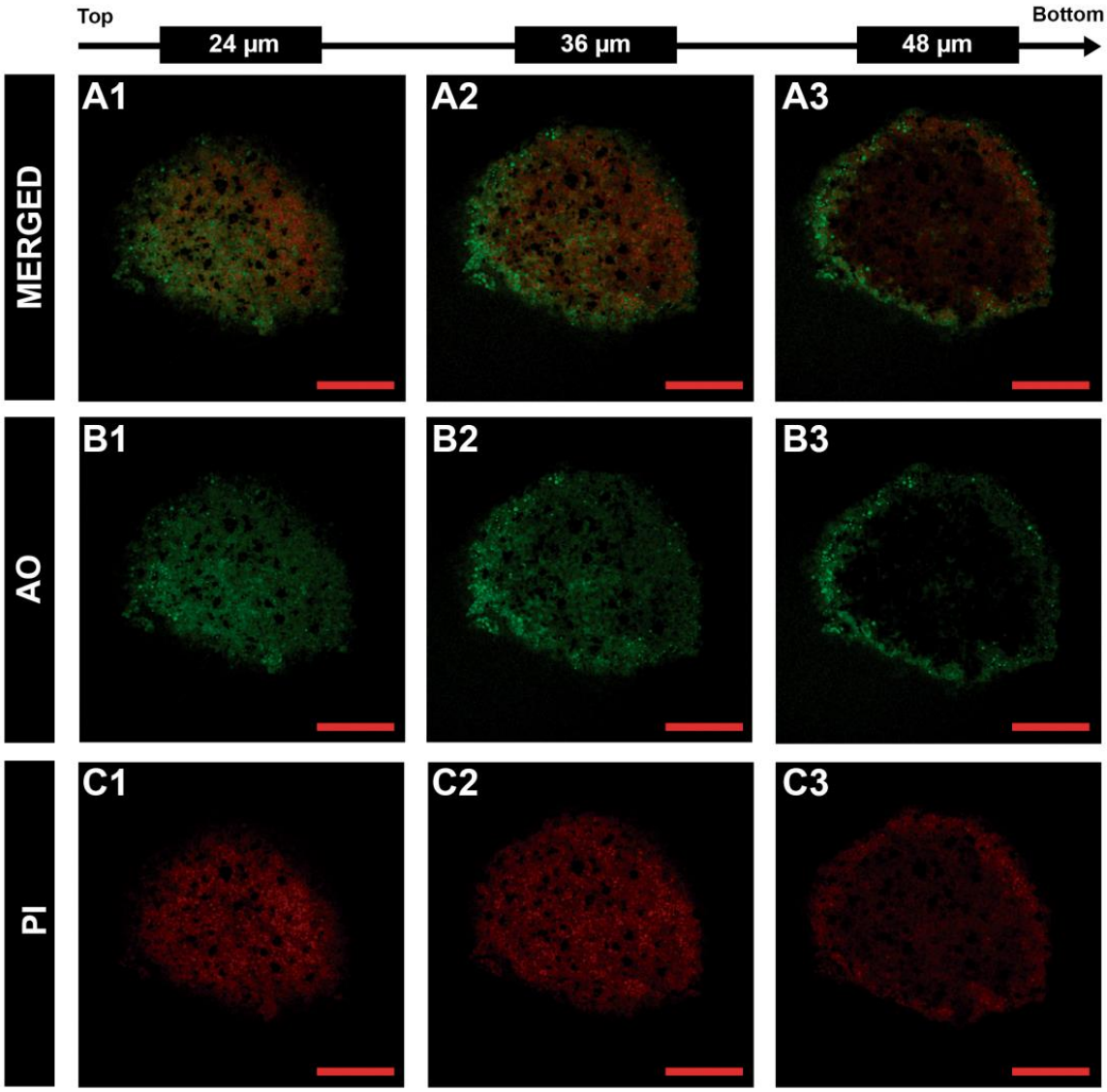

Figure 16. CLSM images of 3MCF-7:1NHDF spheroids after 9 days of cells (100000 cells/well) being seeded on 96-well plates coated with HA solution (2.0 mg/mL). (A-C) Z-stack slides of spheroids at different penetration depth (24, 36 and 48 µm). Green channel - live and necrotic cell stained with AO; RED channel - PI staining the nucleus of necrotic cells; Merged channel- Superimposition of all channels. Scale bar corresponds to 200 µm.

The PI staining was used to highlight the cells that have a compromised cell membrane (red fluorescence), whereas AO cell-permeable probe is selective for nucleic acids, labelling all the cells present in spheroid (green fluorescence). The confocal laser scanning microscopic (CLSM) images of spheroids produced with 100000 cells/well showed a significantly higher amount of necrotic cells in the spheroid core (Figure 16 C), while most of the cells at the periphery remain non-necrotic (Figure 16 B). The establishment of this cellular microenvironment within the spheroid shows that they have a cellular distribution similar to that found in real breast tumors [102].

Chapter IV

Conclusions and Future Perspectives

4. Conclusions and Future Perspectives

Despite the huge efforts performed in the area of cancer research, the currently available anticancer therapies often do not have the desired therapeutic efficacy and also trigger side effects for patients. To surpass such limitations, new therapies are highly demand.

Currently, 2D cell culture is the main methodology used for screening new anticancer therapeutics due to its easy handling and low cost. However, this system is unable to mimic the major features of solid tumors, such as, the 3D structure, cell-cell and cell-ECM interactions that have an essential role in tumor progression. On the other hand, the use of *in vivo* systems is associated with economical and ethical issues. Thus, to overcome these problems, the researchers started to develop *in vitro* 3D tumor models that are able to represent the main features of human solid tumors, namely spheroids.

So far, different methods have been applied for spheroids assembly, namely LOT. In a previous study form our group it was optimized this technique to assemble heterotypic breast cancer spheroids on a non-adherent biomaterial (agarose). However, spheroids assembled on surfaces coated with agarose are not able to represent the cells-ECM interactions. Therefore, in this thesis, it was optimized for the first time the reproducible assembly of 3D heterotypic breast cancer spheroids on HA-coated surfaces by using different HA concentrations and initial cell-seeding numbers. The produced 3D models were able to represent cells-HA interactions, and also other features found in *in vivo* breast cancers, such as cellular heterogeneity, cell-cell physical interactions and the presence of a dense and necrotic region in the center of the spheroids.

Additionally, it was also shown that the size, number and morphology of the spheroids can also be modulated by changing the HA concentration and the initial cell number used. In general, the increase of HA concentration and cell-seeding density leads to the attainment of spherical-like spheroids with larger diameters (> 500 μm), which better represent the main features of solid tumors.

In conclusion, it was possible to promote the assembly of breast cancer spheroids, on HA-coated surfaces, that are capable of mimicking the complex microenvironment of solid tumors. Furthermore, one of the main achievements of this work was the formation of spheroids in contact with an ECM element, which is known to have an essential role in tumor progression, since it is responsible for the establishment of interactions with cells surface receptors that will promote the transducing of intracellular signals involved in cells differentiation, survival, proliferation, migration, angiogenesis and resistance to therapeutic molecules.

The use of these simple and inexpensive 3D models to evaluate the biological performance of anticancer therapies will allow the obtainment of more accurate results than those obtained with 2D cell cultures, since spheroids are able to better reproduce the complexity of tumor microenvironment. In the near future, these HA-coated surfaces can be used not only for assembly 3D cancer models to be used for drug screening, but also to study the cell-HA interactions that are established *in vivo* and that give a huge contribute for tumor progression (*e.g.*, promotion of cells proliferation and migration). Moreover the cell therapeutics resistance mechanisms may as well be studied in further detail.

Chapter V

References

5. References

1. Mross, K. and F. Kratz, *Limits of Conventional Cancer Chemotherapy*, in *Drug Delivery in Oncology*. 2011, Wiley-VCH Verlag GmbH & Co. KGaA. 1-31.

2. Yamada, K.M. and E. Cukierman, *Modeling Tissue Morphogenesis and Cancer in 3D*. Cell, 2007. 130: 601-610.

3. Ledford, H., *US cancer institute to overhaul tumour cell lines*. Nature, 2016. 530: 391.

4. Bhadriraju, K. and C.S. Chen, *Engineering cellular microenvironments to improve cell-based drug testing*. Drug Discovery Today, 2002. 7: 612-620.

5. Mehta, G., A.Y. Hsiao, M. Ingram, G.D. Luker, and S. Takayama, *Opportunities and challenges for use of tumor spheroids as models to test drug delivery and efficacy*. Journal of Controlled Release, 2012. 164: 192-204.

6. Fennema, E., N. Rivron, J. Rouwkema, C. van Blitterswijk, and J. de Boer, *Spheroid culture as a tool for creating 3D complex tissues*. Trends in biotechnology, 2013. 31: 108-115.

7. Kim, J.W., W.J. Ho, and B.M. Wu, *The role of the 3D environment in hypoxia-induced drug and apoptosis resistance*. Anticancer Research, 2011. 31: 3237-3245.

8. Sasaki, T., M. Yamamoto, T. Yamaguchi, and S. Sugiyama, *Development of multicellular spheroids of HeLa cells cocultured with fibroblasts and their response to X-irradiation*. Cancer Research, 1984. 44: 345-351.

9. Timmins, N.E. and L.K. Nielsen, *Generation of multicellular tumor spheroids by the hanging-drop method*. Tissue Engineering, 2007. 140: 141-151.

10. Costa, E.C., V.M. Gaspar, P. Coutinho, and I.J. Correia, *Optimization of liquid overlay technique to formulate heterogenic 3D co-cultures models*. Biotechnology and Bioengineering, 2014. 111: 1672-1685.

11. Wu, L.Y., D. Di Carlo, and L.P. Lee, *Microfluidic self-assembly of tumor spheroids for anticancer drug discovery*. Biomedical Microdevices, 2008. 10: 197-202.

12. Toole, B.P., *Hyaluronan: from extracellular glue to pericellular cue*. Nature Reviews Cancer, 2004. 4: 528-539.

13. Auvinen, P., R. Tammi, J. Parkkinen, M. Tammi, U. Agren, R. Johansson, P. Hirvikoski, M. Eskelinen, and V.M. Kosma, *Hyaluronan in peritumoral stroma and malignant cells associates with breast cancer spreading and predicts survival*. American Journal of Pathology, 2000. 156: 529-536.

14. Ahrens, T., V. Assmann, C. Fieber, C. Termeer, P. Herrlich, M. Hofmann, and J.C. Simon, *CD44 is the principal mediator of hyaluronic-acid-induced melanoma cell proliferation*. Journal of Investigative Dermatology, 2001. 116: 93-101.

15. Kim, H.-R., M.A. Wheeler, C.M. Wilson, J. Iida, D. Eng, M.A. Simpson, J.B. McCarthy, and K.M. Bullard, *Hyaluronan facilitates invasion of colon carcinoma cells in vitro via interaction with CD44*. Cancer Research, 2004. 64: 4569-4576.

16. Kouvidi, K., A. Berdiaki, D. Nikitovic, P. Katonis, N. Afratis, V.C. Hascall, N.K. Karamanos, and G.N. Tzanakakis, *Role of receptor for hyaluronic acid-mediated*

motility (RHAMM) in low molecular weight hyaluronan (LMWHA)-mediated fibrosarcoma cell adhesion. Journal of Biological Chemistry, 2011. 286: 38509-38520.

17. Laurich, C., M.A. Wheeler, J. Iida, C.L. Neudauer, J.B. McCarthy, and K.M. Bullard, *Hyaluronan mediates adhesion of metastatic colon carcinoma cells 1.* Journal of Surgical Research, 2004. 122: 70-74.

18. Misra, S., S. Ghatak, A. Zoltan-Jones, and B.P. Toole, *Regulation of multidrug resistance in cancer cells by hyaluronan.* Journal of Biological Chemistry, 2003. 278: 25285-25288.

19. Vincent, T., M. Jourdan, M.-S. Sy, B. Klein, and N. Mechti, *Hyaluronic Acid Induces Survival and Proliferation of Human Myeloma Cells through an Interleukin-6-mediated Pathway Involving the Phosphorylation of Retinoblastoma Protein.* Journal of Biological Chemistry, 2001. 276: 14728-14736.

20. Zhang, L., C.B. Underhill, and L. Chen, *Hyaluronan on the surface of tumor cells is correlated with metastatic behavior.* Cancer Research, 1995. 55: 428-433.

21. Zhang, Y., A.A. Thant, K. Machida, Y. Ichigotani, Y. Naito, et al., *Hyaluronan-CD44s signaling regulates matrix metalloproteinase-2 secretion in a human lung carcinoma cell line QG90.* Cancer Research, 2002. 62: 3962-3965.

22. Anttila, M.A., R.H. Tammi, M.I. Tammi, K.J. Syrjänen, S.V. Saarikoski, and V.-M. Kosma, *High Levels of Stromal Hyaluronan Predict Poor Disease Outcome in Epithelial Ovarian Cancer.* Cancer Research, 2000. 60: 150-155.

23. David, L., V. Dulong, D. Le Cerf, C. Chauzy, V. Norris, B. Delpech, M. Lamacz, and J.P. Vannier, *Reticulated hyaluronan hydrogels: a model for examining cancer cell invasion in 3D.* Matrix Biology, 2004. 23: 183-193.

24. Khademhosseini, A., K.Y. Suh, J.M. Yang, G. Eng, J. Yeh, S. Levenberg, and R. Langer, *Layer-by-layer deposition of hyaluronic acid and poly-L-lysine for patterned cell co-cultures.* Biomaterials, 2004. 25: 3583-3592.

25. Pavesio, A., D. Renier, C. Cassinelli, and M. Morra, *Anti-adhesive surfaces through hyaluronan coatings.* Medical Device Technologies, 1997. 8: 20-1, 24-7.

26. Li, L., Y. Qian, C. Jiang, Y. Lv, W. Liu, L. Zhong, K. Cai, S. Li, and L. Yang, *The use of hyaluronan to regulate protein adsorption and cell infiltration in nanofibrous scaffolds.* Biomaterials, 2012. 33: 3428-3445.

27. Ghatak, S., S. Misra, and B.P. Toole, *Hyaluronan oligosaccharides inhibit anchorage-independent growth of tumor cells by suppressing the phosphoinositide 3-kinase/Akt cell survival pathway.* Journal of Biological Chemistry, 2002. 277: 38013-38020.

28. Vara, J.Á.F., E. Casado, J. de Castro, P. Cejas, C. Belda-Iniesta, and M. González-Barón, *PI3K/Akt signalling pathway and cancer.* Cancer Treatment Reviews, 2004. 30: 193-204.

29. Osaki, M., M. Oshimura, and H. Ito, *PI3K-Akt pathway: Its functions and alterations in human cancer.* Apoptosis. 9: 667-676.

30. Bourguignon, L.Y., G. Wong, C. Earle, K. Krueger, and C.C. Spevak, *Hyaluronan-CD44 interaction promotes c-Src-mediated twist signaling, microRNA-10b expression, and RhoA/RhoC up-regulation, leading to Rho-kinase-associated cytoskeleton activation and breast tumor cell invasion.* Journal of Biological Chemistry, 2010. 285: 36721-36735.

31. Je, E.-C., B.S. Lca, and G.A. Ga, *The role of transcription factor TWIST in cancer cells.* Journal of Genetic Syndromes & Gene therapy, 2013. 4: 1-7.

32. Hamilton, S.R., S.F. Fard, F.F. Paiwand, C. Tolg, M. Veiseh, et al., *The hyaluronan receptors CD44 and Rhamm (CD168) form complexes with ERK1,2 that sustain high basal motility in breast cancer cells.* Journal of Biological Chemistry, 2007. 282: 16667-16680.

33. Bourguignon, L.Y., H. Zhu, L. Shao, and Y.W. Chen, *CD44 interaction with tiam1 promotes Rac1 signaling and hyaluronic acid-mediated breast tumor cell migration.* Journal of Biological Chemistry, 2000. 275: 1829-1838.

34. Park, M.-J., M.-S. Kim, I.-C. Park, H.-S. Kang, H. Yoo, S.H. Park, C.H. Rhee, S.-I. Hong, and S.-H. Lee, *PTEN Suppresses Hyaluronic Acid-induced Matrix Metalloproteinase-9 Expression in U87MG Glioblastoma Cells through Focal Adhesion Kinase Dephosphorylation.* Cancer Research, 2002. 62: 6318-6322.

35. Lokeshwar, V.B., S. Mirza, and A. Jordan, *Targeting hyaluronic acid family for cancer chemoprevention and therapy.* Advances in Cancer Research, 2014. 123: 35-65.

36. Misra, S., P. Ujházy, L. Varticovski, and I.M. Arias, *Phosphoinositide 3-kinase lipid products regulate ATP-dependent transport by sister of P-glycoprotein and multidrug resistance associated protein 2 in bile canalicular membrane vesicles.* Proceedings of the National Academy of Sciences of the United States of America, 1999. 96: 5814-5819.

37. Bourguignon, L.Y., G. Wong, C. Earle, and L. Chen, *Hyaluronan-CD44v3 interaction with Oct4-Sox2-Nanog promotes miR-302 expression leading to self-renewal, clonal formation, and cisplatin resistance in cancer stem cells from head and neck squamous cell carcinoma.* Journal of Biological Chemistry, 2012. 287: 32800-32824.

38. Florczyk, S.J., K. Wang, S. Jana, D.L. Wood, S.K. Sytsma, J.G. Sham, F.M. Kievit, and M. Zhang, *Porous chitosan-hyaluronic acid scaffolds as a mimic of glioblastoma microenvironment ECM.* Biomaterials, 2013. 34: 10143-10150.

39. Huang, Y.-J. and S.-h. Hsu, *Acquisition of epithelial-mesenchymal transition and cancer stem-like phenotypes within chitosan-hyaluronan membrane-derived 3D tumor spheroids.* Biomaterials, 2014. 35: 10070-10079.

40. Dean, M., T. Fojo, and S. Bates, *Tumour stem cells and drug resistance.* Nature Reviews Cancer, 2005. 5: 275-284.

41. Pan, T., E.L. Fong, M. Martinez, D.A. Harrington, S.-H. Lin, M.C. Farach-Carson, and R.L. Satcher, *Three-dimensional (3d) culture of bone-derived human 786-o renal cell carcinoma retains relevant clinical characteristics of bone metastases.* Cancer Letters, 2015. 365: 89-95.

42. Bourguignon, L.Y., H. Zhu, L. Shao, and Y.W. Chen, *CD44 interaction with c-Src kinase promotes cortactin-mediated cytoskeleton function and hyaluronic acid-dependent ovarian tumor cell migration.* Journal of Biological Chemistry, 2001. 276: 7327-7336.

43. Hanagiri, T., S. Shinohara, M. Takenaka, Y. Shigematsu, M. Yasuda, et al., *Effects of hyaluronic acid and CD44 interaction on the proliferation and invasiveness of malignant pleural mesothelioma.* Tumor Biology, 2012. 33: 2135-2141.

44. Misra, S., S. Ghatak, A. Zoltan-Jones, and B.P. Toole, *Regulation of MDR1 Expression and Drug Resistance by a Positive Feedback Loop Involving Hyaluronan, Phosphoinositide 3-Kinase, and ErbB2.* Journal of Biological Chemistry, 2005. 280: 20310-20315.

45. Wang, S.J. and L.Y. Bourguignon, *Hyaluronan-CD44 promotes phospholipase C-mediated Ca2+ signaling and cisplatin resistance in head and neck cancer.* Archives of Otolaryngology - Head and Neck Surgery, 2006. 132: 19-24.

46. Ohashi, R., F. Takahashi, R. Cui, M. Yoshioka, T. Gu, et al., *Interaction between CD44 and hyaluronate induces chemoresistance in non-small cell lung cancer cell.* Cancer Letters, 2007. 252: 225-234.

47. David, L., V. Dulong, D. Le Cerf, L. Cazin, M. Lamacz, and J.P. Vannier, *Hyaluronan hydrogel: an appropriate three-dimensional model for evaluation of anticancer drug sensitivity.* Acta Biomaterialia, 2008. 4: 256-263.

48. Turley, E.A., P.W. Noble, and L.Y. Bourguignon, *Signaling properties of hyaluronan receptors.* Journal of Biological Chemistry, 2002. 277: 4589-4592.

49. Erickson, M. and R. Stern, *Chain gangs: new aspects of hyaluronan metabolism.* Biochemistry Research International, 2011. 2012: 1-9.

50. Yang, C., M. Cao, H. Liu, Y. He, J. Xu, et al., *The High and Low Molecular Weight Forms of Hyaluronan Have Distinct Effects on CD44 Clustering.* The Journal of Biological Chemistry, 2012. 287: 43094-43107.

51. Zeng, C., B.P. Toole, S.D. Kinney, J.W. Kuo, and I. Stamenkovic, *Inhibition of tumor growth in vivo by hyaluronan oligomers.* International Journal of Cancer, 1998. 77: 396-401.

52. Afify, A., P. Purnell, and L. Nguyen, *Role of CD44s and CD44v6 on human breast cancer cell adhesion, migration, and invasion.* Experimental and Molecular Pathology, 2009. 86: 95-100.

53. Carlsson, J. and J.M. Yuhas, *Liquid-Overlay Culture of Cellular Spheroids*, in *Spheroids in Cancer Research*, H. Acker, et al., Editors. 1984, Springer Berlin Heidelberg. 1-23.

54. Ratnayaka, S.H., T.E. Hillburn, O. Forouzan, S.S. Shevkoplyas, and D.B. Khismatullin, *PDMS well platform for culturing millimeter-size tumor spheroids.* Biotechnology Progress, 2013. 29: 1265-1269.

55. Chauzy, C., B. Delpech, A. Olivier, C. Bastard, N. Girard, et al., *Establishment and characterisation of a human glioma cell line.* European Journal of Cancer, 1992. 28: 1129-1134.

56. Stark, Y., S. Bruns, F. Stahl, C. Kasper, M. Wesemann, C. Grothe, and T. Scheper, *A study on polysialic acid as a biomaterial for cell culture applications.* Journal of Biomedical Materials Research Part A, 2008. 85: 1-13.

57. Xu, K., K. Narayanan, F. Lee, K.H. Bae, S. Gao, and M. Kurisawa, *Enzyme-mediated hyaluronic acid-tyramine hydrogels for the propagation of human embryonic stem cells in 3D.* Acta Biomaterialia, 2015. 24: 159-171.

58. Lai, J.-Y. and I.-H. Tu, *Adhesion, phenotypic expression, and biosynthetic capacity of corneal keratocytes on surfaces coated with hyaluronic acid of different molecular weights.* Acta Biomaterialia, 2012. 8: 1068-1079.

59. Nguyen, K.T. and J.L. West, *Photopolymerizable hydrogels for tissue engineering applications.* Biomaterials, 2002. 23: 4307-4314.

60. Burdick, J.A. and G.D. Prestwich, *Hyaluronic acid hydrogels for biomedical applications.* Advanced Materials, 2011. 23: H41-H56.

61. Collins, M.N. and C. Birkinshaw, *Hyaluronic acid based scaffolds for tissue engineering—A review.* Carbohydrate Polymers, 2013. 92: 1262-1279.

62. Prestwich, G.D., D.M. Marecak, J.F. Marecek, K.P. Vercruysse, and M.R. Ziebell, *Controlled chemical modification of hyaluronic acid: synthesis, applications, and biodegradation of hydrazide derivatives.* Journal of Controlled Release, 1998. 53: 93-103.

63. Gurski, L.A., A.K. Jha, C. Zhang, X. Jia, and M.C. Farach-Carson, *Hyaluronic acid-based hydrogels as 3D matrices for in vitro evaluation of chemotherapeutic drugs using poorly adherent prostate cancer cells.* Biomaterials, 2009. 30: 6076-6085.

64. Xu, X., L.A. Gurski, C. Zhang, D.A. Harrington, M.C. Farach-Carson, and X. Jia, *Recreating the tumor microenvironment in a bilayer, hyaluronic acid hydrogel construct for the growth of prostate cancer spheroids.* Biomaterials, 2012. 33: 9049-9060.

65. Chung, C., M. Beecham, R.L. Mauck, and J.A. Burdick, *The Influence of Degradation Characteristics of Hyaluronic Acid Hydrogels on In Vitro Neocartilage Formation by Mesenchymal Stem Cells.* Biomaterials, 2009. 30: 4287-4296.

66. Jeon, O., S.J. Song, K.-J. Lee, M.H. Park, S.-H. Lee, S.K. Hahn, S. Kim, and B.-S. Kim, *Mechanical properties and degradation behaviors of hyaluronic acid hydrogels cross-linked at various cross-linking densities.* Carbohydrate Polymers, 2007. 70: 251-257.

67. Ji, Y., K. Ghosh, X.Z. Shu, B. Li, J.C. Sokolov, G.D. Prestwich, R.A. Clark, and M.H. Rafailovich, *Electrospun three-dimensional hyaluronic acid nanofibrous scaffolds.* Biomaterials, 2006. 27: 3782-3792.

68. Um, I.C., D. Fang, B.S. Hsiao, A. Okamoto, and B. Chu, *Electro-Spinning and Electro-Blowing of Hyaluronic Acid.* Biomacromolecules, 2004. 5: 1428-1436.

69. Kim, I.L., S. Khetan, B.M. Baker, C.S. Chen, and J.A. Burdick, *Fibrous hyaluronic acid hydrogels that direct MSC chondrogenesis through mechanical and adhesive cues.* Biomaterials, 2013. 34: 5571-5580.

70. Wang, Y. and J. Wang, *Mixed hydrogel bead-based tumor spheroid formation and anticancer drug testing.* Analyst, 2014. 139: 2449-2458.

71. Bae, K.H., J.J. Yoon, and T.G. Park, *Fabrication of hyaluronic acid hydrogel beads for cell encapsulation.* Biotechnology Progress, 2006. 22: 297-302.

72. Skardal, A., S.F. Sarker, A. Crabbé, C.A. Nickerson, and G.D. Prestwich, *The generation of 3-D tissue models based on hyaluronan hydrogel-coated microcarriers within a rotating wall vessel bioreactor.* Biomaterials, 2010. 31: 8426-8435.

73. Huang, G.S., L.G. Dai, B.L. Yen, and S.H. Hsu, *Spheroid formation of mesenchymal stem cells on chitosan and chitosan-hyaluronan membranes.* Biomaterials, 2011. 32: 6929-6945.

74. Hsu, S.H. and G.S. Huang, *Substrate-dependent Wnt signaling in MSC differentiation within biomaterial-derived 3D spheroids.* Biomaterials, 2013. 34: 4725-4738.

75. Polyak, K., *Heterogeneity in breast cancer.* The Journal of Clinical Investigation, 2011. 121: 3786-3788.

76. Costa, E.C., V.M. Gaspar, J.G. Marques, P. Coutinho, and I.J. Correia, *Evaluation of nanoparticle uptake in co-culture cancer models.* PLoS ONE, 2013. 8: e70072.

77. Schneider, C.A., W.S. Rasband, and K.W. Eliceiri, *NIH Image to ImageJ: 25 years of image analysis.* Nature Methods, 2012. 9: 671-675.

78. Castells, M., B. Thibault, J.-P. Delord, and B. Couderc, *Implication of tumor microenvironment in chemoresistance: tumor-associated stromal cells protect tumor cells from cell death.* International Journal of Molecular Sciences, 2012. 13: 9545-9571.

79. Miki, Y., K. Ono, S. Hata, T. Suzuki, H. Kumamoto, and H. Sasano, *The advantages of co-culture over mono cell culture in simulating in vivo environment.* The Journal of Steroid Biochemistry and Molecular Biology, 2012. 131: 68-75.

80. Cirri, P. and P. Chiarugi, *Cancer-associated-fibroblasts and tumour cells: a diabolic liaison driving cancer progression.* Cancer and Metastasis Reviews, 2012. 31: 195-208.

81. Estrada, M.F., S.P. Rebelo, E.J. Davies, M.T. Pinto, H. Pereira, et al., *Modelling the tumour microenvironment in long-term microencapsulated 3D co-cultures recapitulates phenotypic features of disease progression.* Biomaterials, 2016. 78: 50-61.

82. Martinez-Outschoorn, U.E., Z. Lin, Y.-H. Ko, A. Goldberg, N. Flomenberg, et al., *Understanding the metabolic basis of drug resistance: therapeutic induction of the Warburg effect kills cancer cells.* Cell Cycle, 2011. 10: 2521-2528.

83. Sabhachandani, P., V. Motwani, N. Cohen, S. Sarkar, V. Torchilin, and T. Konry, *Generation and Functional Assessment of 3D Multicellular Spheroids in droplet based Microfluidics Platform.* Lab on a Chip, 2016. 16: 497-505.

84. Minchinton, A.I. and I.F. Tannock, *Drug penetration in solid tumours.* Nature Reviews Cancer, 2006. 6: 583-592.

85. Godugu, C., A.R. Patel, U. Desai, T. Andey, A. Sams, and M. Singh, *AlgiMatrix™ Based 3D Cell Culture System as an In-Vitro Tumor Model for Anticancer Studies.* PLoS ONE, 2013. 8: e53708.

86. West, C., *Size-dependent resistance of human tumour spheroids to photodynamic treatment.* British Journal of Cancer, 1989. 59: 510-514.

87. LaBarbera, D.V., B.G. Reid, and B.H. Yoo, *The multicellular tumor spheroid model for high-throughput cancer drug discovery.* Expert Opinion on Drug Discovery, 2012. 7: 819-830.

88. Ma, H.-l., Q. Jiang, S. Han, Y. Wu, J.C. Tomshine, D. Wang, Y. Gan, G. Zou, and X.-J. Liang, *Multicellular tumor spheroids as an in vivo-like tumor model for three-dimensional imaging of chemotherapeutic and nano material cellular penetration.* Molecular Imaging, 2012. 11: 487-498.

89. Cheng, G., J. Tse, R.K. Jain, and L.L. Munn, *Micro-environmental mechanical stress controls tumor spheroid size and morphology by suppressing proliferation and inducing apoptosis in cancer cells.* PLoS ONE, 2009. 4: e4632.

90. Hirschhaeuser, F., H. Menne, C. Dittfeld, J. West, W. Mueller-Klieser, and L.A. Kunz-Schughart, *Multicellular tumor spheroids: an underestimated tool is catching up again.* Journal of Biotechnology, 2010. 148: 3-15.

91. Ivascu, A. and M. Kubbies, *Rapid generation of single-tumor spheroids for high-throughput cell function and toxicity analysis.* Journal of Biomolecular Screening, 2006. 11: 922-932.

92. Kim, J.B., *Three-dimensional tissue culture models in cancer biology.* Seminars in Cancer Biology, 2005. 15: 365-377.

93. Kalluri, R. and M. Zeisberg, *Fibroblasts in cancer*. Nature Reviews Cancer, 2006. 6: 392-401.

94. Chou, S.-F., J.-Y. Lai, C.-H. Cho, and C.-H. Lee, *Relationships between surface roughness/stiffness of chitosan coatings and fabrication of corneal keratocyte spheroids: Effect of degree of deacetylation*. Colloids and Surfaces B: Biointerfaces, 2016. 142: 105-113.

95. Shin, C., B. Kwak, B. Han, and K. Park, *3D cancer tumor models for evaluating chemotherapeutic efficacy*, in *Biomaterials for Cancer Therapeutics: Diagnosis, Prevention and Therapy*, K. Park, Editor. 2013, Woodhead Publishing. 445-460.

96. Tannock, I.F., C.M. Lee, J.K. Tunggal, D.S. Cowan, and M.J. Egorin, *Limited penetration of anticancer drugs through tumor tissue a potential cause of resistance of solid tumors to chemotherapy*. Clinical Cancer Research, 2002. 8: 878-884.

97. Gaspar, V.M., E.C. Costa, J.A. Queiroz, C. Pichon, F. Sousa, and I.J. Correia, *Folate-targeted multifunctional amino acid-chitosan nanoparticles for improved cancer therapy*. Pharmaceutical Research, 2014. 32: 562-577.

98. Trédan, O., C.M. Galmarini, K. Patel, and I.F. Tannock, *Drug resistance and the solid tumor microenvironment*. Journal of the National Cancer Institute 2007. 99: 1441-1454.

99. Wrzesinski, K. and S.J. Fey, *After trypsinisation, 3D spheroids of C3A hepatocytes need 18 days to re-establish similar levels of key physiological functions to those seen in the liver*. Toxicology Research, 2013. 2: 123-135.

100. Gong, X., C. Lin, J. Cheng, J. Su, H. Zhao, T. Liu, X. Wen, and P. Zhao, *Generation of Multicellular Tumor Spheroids with Microwell-Based Agarose Scaffolds for Drug Testing*. PLoS ONE, 2015. 10: e0130348.

101. Desoize, B. and J.-C. Jardillier, *Multicellular resistance: a paradigm for clinical resistance?* Critical Reviews in Oncology/Hematology, 2000. 36: 193-207.

102. Rundqvist, H. and R.S. Johnson, *Tumour oxygenation: implications for breast cancer prognosis*. Journal of Internal Medicine, 2013. 274: 105-112.